THE 1989 PRESTRESSED GIRDER PROJECT

Principle Investigator:

Dr. Arden B. Sigl, P.E.
Civil Engineering Department

Final Report
June 1990

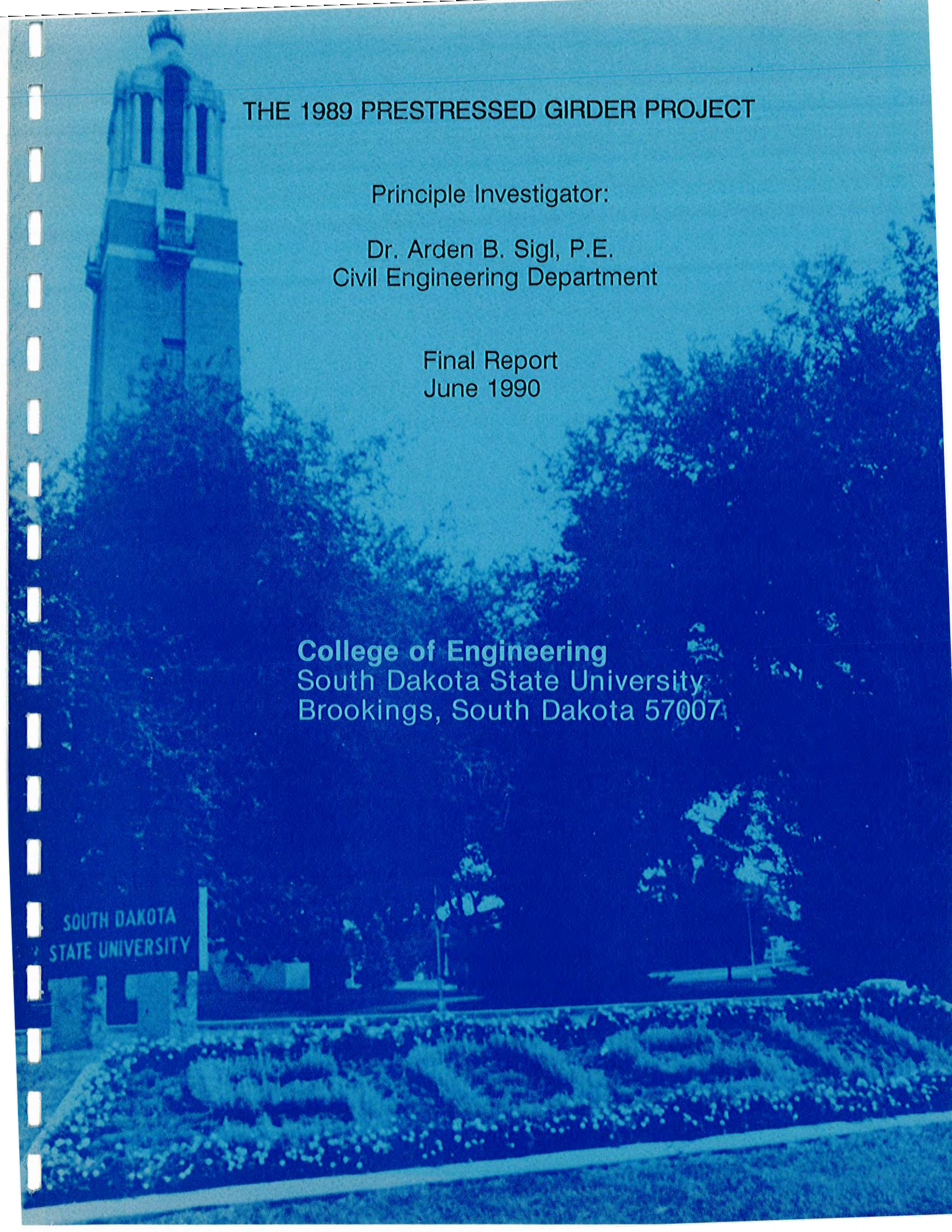

College of Engineering
South Dakota State University
Brookings, South Dakota 57007

THE 1989 PRESTRESSED GIRDER PROJECT

Principle Investigator:

Prof. Arden B. Sigl, Ph.D., P.E.
Civil Engineering Department
South Dakota State University

Contracting Agency:

South Dakota Department of Transportation
and State Transportation Commission
for Division of Highways

June 1990

Final Report

Agreement No. 3369

ACKNOWLEDGEMENT

The contents of this report reflect the view of the author who is responsible for the facts and the accuracy of the data presented herein. The contents do not necessarily reflect the official views of policies of the South Dakota Department of Transportation, the State Transportation Commission, or the U.S. Federal Highway Administration. This report does not constitute a standard specification, or regulation.

The writer wants to thank the individuals at the SDDOT who cooperated with him during this project. The inspection and load testing phase of the project required the commitment of personnel and equipment at the required times in order to allow the project to proceed on schedule. This support was readily provided as requested.

The writer also wishes to recognize the assistance in the form of quick responses to requests and questions, by Ms. Laurie Schultz and Mr. David Huft.

The writer recognizes the excellent assistance provided by Mr. Bob Szrot who was the graduate student that worked on the project.

Arden B. Sigl, Ph.D., P.E.
Professor of Civil Engineering

TABLE OF CONTENTS

LIST OF TABLES

LIST OF FIGURES

1.0 Introduction.

In January of 1989 personnel of the South Dakota Department of Transportation discovered that the 18th Street Bridge in Sioux Falls, South Dakota, which was under contract for deck removal and widening, had longitudinal full length cracks in several of its girders. This bridge is a prestressed girder bridge having a cast in place reinforced concrete composite deck. The crack was discovered after the deck had been partially removed in preparation for the widening of the structure. The discovery of this crack prompted the inspection of other prestressed girder bridges that had recently had their decks replaced. The same type of longitudinal crack was found in some of the girders of these structures.

Further inspections were made of several other prestressed girder bridges. These inspections included structures with and without deck replacement. The cracks were also found in some of these structures. These discoveries generated some concern as to the impact of this type of cracking on the life and load carrying capacity of these bridges. The 1989 Prestressed Girder Project was undertaken to provide insight into the cause and probable effect that this cracking will have on the service life of these structures.

1.1 The Project Objectives.

The project had the following objectives:

1. To determine the probable cause of the cracking.
2. To determine if the presence of the crack has reduced the strength of the affected girders.
3. To determine if epoxy injection will effectively repair the girders.

1.2 The Affected Structures.

The affected bridges have prestressed supporting girders with cast in place composite concrete decks. A typical side view of one of these structures is presented in Figure 1. A typical cross section through one of these bridges is given in Figure 2. The prestressed girders are standard AASHTO girders with a typical cross section as presented in Figure 3.

The girders are of precast pretensioned design having bonded tendons. The girder design makes use of both straight and harped tendons. A typical construction sequence consists of precasting and curing the girders in a precasting yard and subsequently transporting them to the site. The girders are put in place, and a composite concrete roadway slab is cast.

The type of cracking, that is the subject of the present study, is a longitudinal crack that occurs in the web portion of the cross section just below the chamfer for the top flange. This crack location is sketched in Figure 3.

1.3 Considerations In the Evaluation Of the Probable Cause Of the Cracking.

Several factors are of interest when considering the cause of the cracking. The 18th Street Bridge (Structure No. 50-214-215) in Sioux Falls, on which the initial discovery was made, is a skewed structure. The two structures which carry I-229 traffic over Cliff Avenue (Structure No.s 50-210-230 and 50-211-230) and exhibit the cracking are skewed structures. Another structure which is known to exhibit the cracking, is the bridge over the Sioux River Diversion Channel on North Minnesota Avenue (Structure No. 50-201-173). This is also a skewed structure. This writer, in preparation for writing the initial proposal for this project, inspected the preceding structures, and in addition,

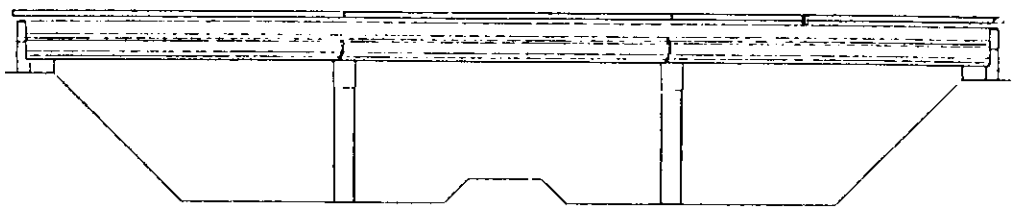

Figure 1. Typical Elevation View

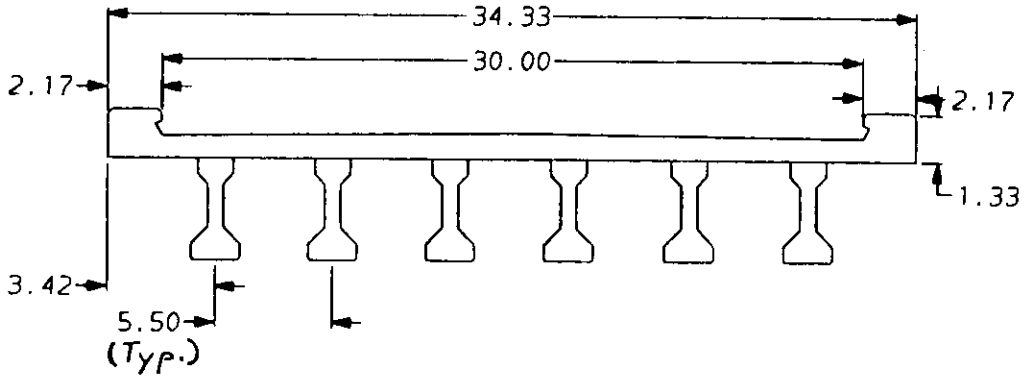

Figure 2. Typical Cross Section
(All Dimensions in Feet)

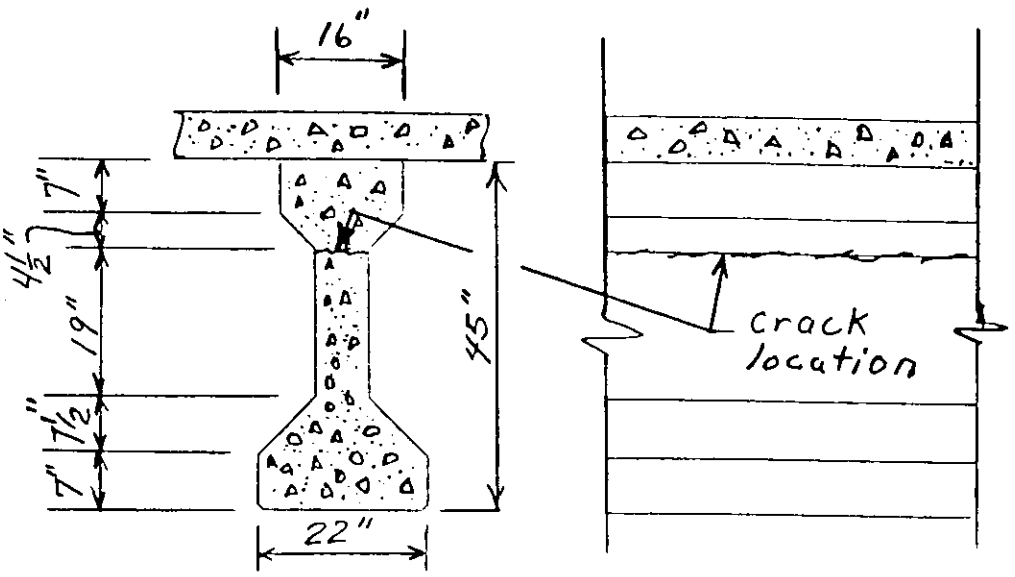

Figure 3. AASHTO TYPE III Girder With Crack Location.

inspected Structure No. 06-185-190. This structure is located three miles south of the Highway 14 and I-90 interchange in Brookings County. This structure has zero skew and based on this preliminary inspection was thought not to exhibit the cracking. Subsequent inspection which was carried out as part of this project indicated that this structure did have a limited amount of hairline cracking. Structure skew was regarded as an important factor in the study of the cause of cracking.

As previously stated, these structures make use of a composite design utilizing concretes of two different ages and strengths. This results in different creep and shrinkage characteristics for the two concretes. This differential shrinkage may be a factor in the cracking.

Some of the structures previously discussed have had their decks replaced and some have not. Deck replacement was discussed as a possible contributing factor to the cracking. Limited preliminary inspection of

structures that had, and had not had deck replacement, showed both classes of structures exhibited the cracking. This condition was considered in the study.

1.4 Project Outline.

In order to achieve the stated objectives it was proposed to make a series of bridge inspections, to select one bridge for instrumenting and load testing, and to make use of computer modeling to augment the field testing. In addition, the literature was surveyed in order to evaluate the suitability of epoxy injection as a means of repairing these cracks. The bridge inspections were completed during June and early July, 1989. The installation of strain transducers on the selected structure was completed in late July and early August. The load test was completed in August of 1989. Data reduction and evaluation of the gathered data was completed during the Fall of 1989 and January of 1990. The draft final report was submitted in early April of 1990.

2.0 Inspections and the Load Test.

2.1 Selection and Inspection of the Bridges.

A selected inventory list of bridges of the type of interest was submitted to the writer. This list included bridges in the Sioux Falls and Brookings area. From this list a group of 15 bridges were selected for inspection. In selecting these bridges primary consideration was given to several factors. As already stated, bridge skew was one of these factors. Another factor considered was structure age. A third factor considered was traffic density. In spite of early concern over the effect of deck replacement, preliminary investigation indicated that the cracking appeared to be independent

of deck replacement. The bridges that were inspected are listed in Table 1. Area maps indicating structure locations are provided in Figure 4. This figure locates the bridges that were located in the immediate Sioux Falls area. Figure 5 gives the locations of the structures that are not in the immediate Sioux Falls area.

Table 1. Bridges Inspected

Structure No.	Simp. Cont.	Spans	Skew	Year Built	ADT	Feature Intersected	Location
50-219-210	S	4	0.0	1959	3370	I229 N	12th St. Overhd.
50-221-170	S	4	0.0	1961	100	I229 N	0.3 S I-90 Interch.
50-173-235	C	4	25L	1981	195	I29 N	1M.W 49-Louise Av.
51-065-050	C	4	0.0	1966	69	I29 N	5 S. Brook. Co.
06-185-190	C	4	0.0	1966	92	I29 N	3 S. US 14 Int.
50-310-093	S	4	45R	1964	1065	Split R. Cr.	0.4 S. Garretson
20-060-271	C	3	0.0	1973	1940	Peg Munk Cr.	0.9 N SD 28 Int.
20-061-271	C	3	0.0	1973	1940	Peg Munk Cr.	0.9 N SD 28 Int.
50-125-168	C	3	0.0	1986	1400	Skunk Cr.	0.6 SE I90&38 Int.
50-189-163	S	3	46R	1961	5165	Bur. N. R.R.	0.9 E I29 Int.
50-189-164	S	3	46R	1961	5165	Bur. N. R.R.	0.9 E I29 Int.
50-200-233	S	4	27L	1959	7500	SD 115	Minn. Av. Int.
50-201-233	S	4	27L	1959	7500	SD 115	Minn. Av. Int.
50-210-230	S	3	27L	1959	5565	Cliff Ave.	Cliff Av. Int.
50-211-230	S	3	27L	1959	5565	Cliff Ave.	Cliff Av. Int.

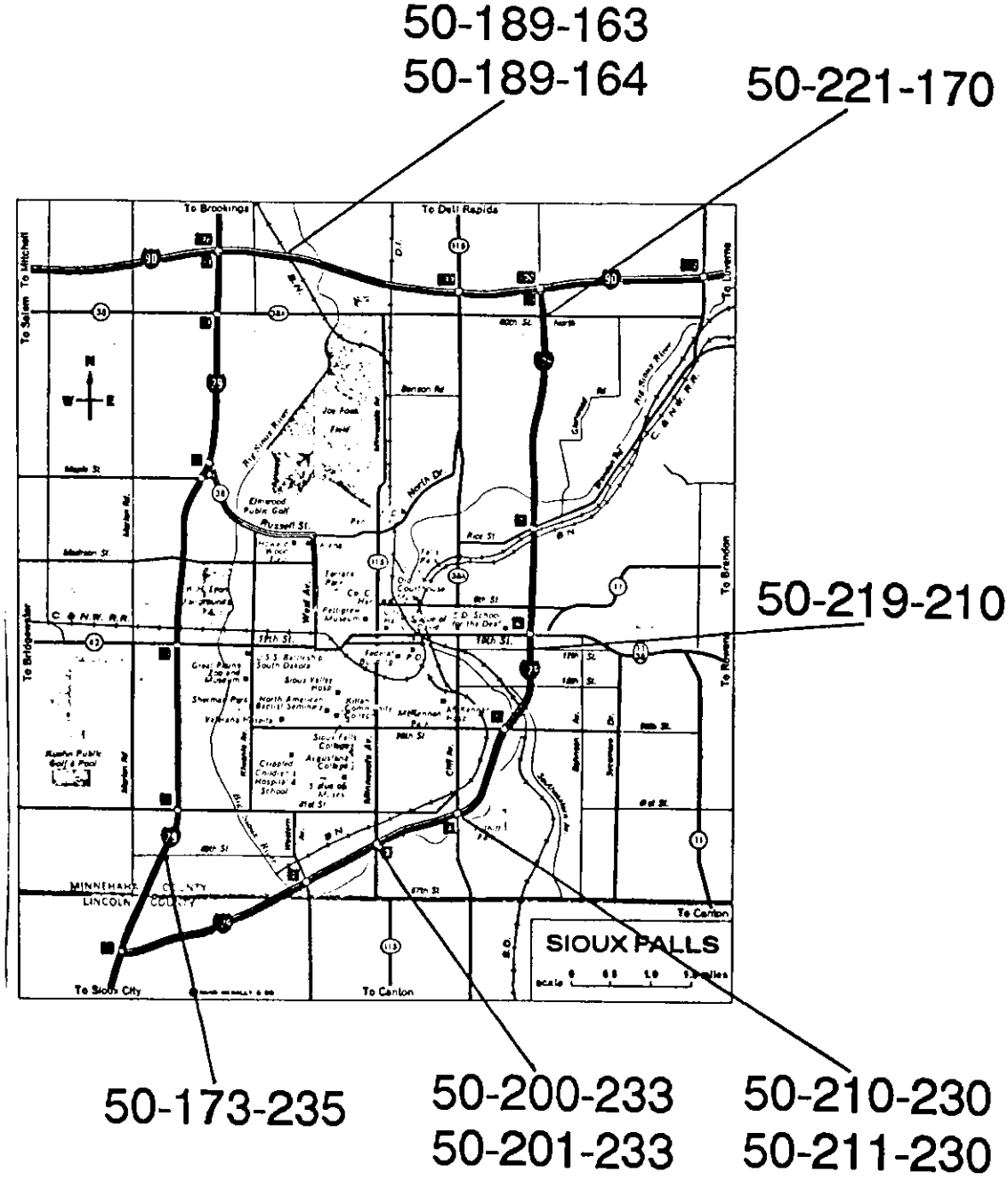

Figure: 4
Bridge Locations Map
Sioux Falls Area

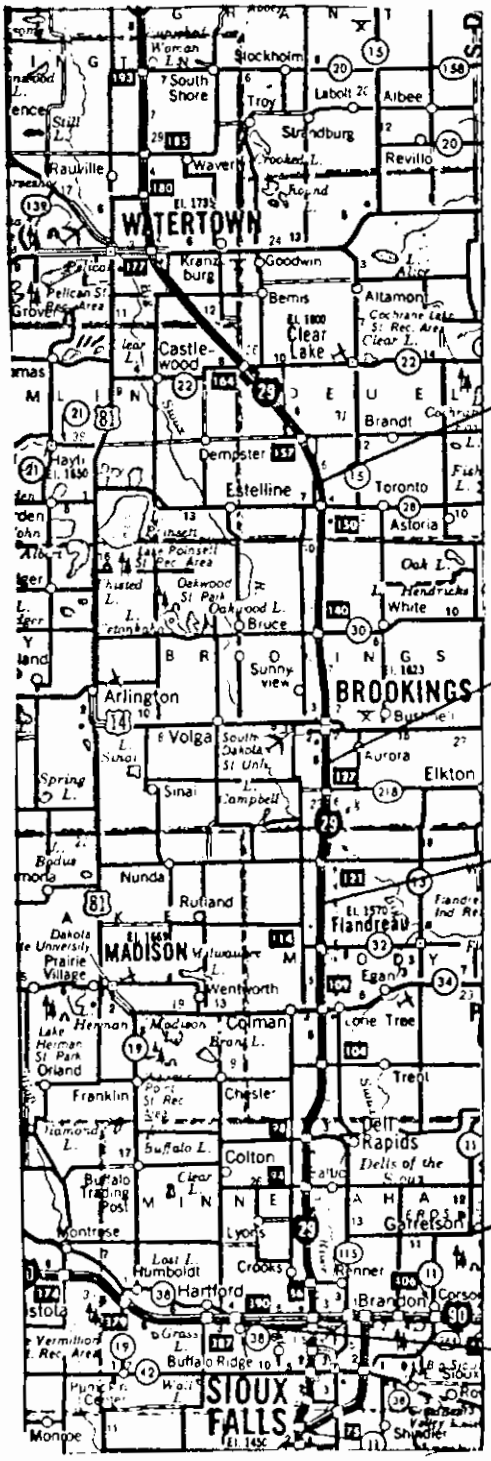

Figure: 5
Bridge Locations Map
Eastern South Dakota

Inspections were conducted out of the Sioux Falls office on June 27, 28, and 29, and out of the Brookings office on July 5. Traffic control was provided by SDDOT. The snooper trucks, one each out of the Sioux Falls and Brookings Offices, were used to provide close inspection of the underside of the bridges. The actual inspections were carried out by the writer and one assistant.

The snooper allowed access across the underside of the bridge transverse to the longitudinal dimension of the structure. Inspections were conducted on both sides of a girder, and typically, at two locations in each span. This procedure typically permitted inspection of all but the last girder across the width. Due to limitations on the reach of the snooper equipment, it was frequently not possible to complete the inspection of the outside girder in the span. Also, practical difficulties of traffic control frequently prevented the inspection at the center of the span.

A typical inspection went as follows. One person concentrated his efforts in the two end spans of the bridge in the region where the earth embankment prevented close inspection with the snooper equipment. A second individual worked from the snooper equipment. Crack width and continuity were noted on both sides of the girder. In order to maintain consistency between the two inspectors, periodically the two individuals would review each others inspection procedures. In addition to the inspection of the cracks, span lengths, bridge width, and girder spacing were routinely measured. These techniques provided both qualitative and subjective data concerning the observed cracks.

2.2 The Instrumented Bridge.

A major focus of this project was the instrumenting and load testing of a bridge that exhibited cracking of the type under study. Suggestions for the bridge to be instrumented were sought from the SDDOT. After consideration of preliminary inspection results and upon recommendation from the SDDOT, structure number, 50-189-164, was selected to be instrumented and load tested. This structure is located on I-90 about 0.9 miles east of the I-90 and I-29 Interchange. It carries east-bound traffic on I-90 over the Burlington Northern Railroad. The location of this structure can be noted by referring to Figure 4.

This bridge, constructed in 1961, consists of three simple spans having span lengths, center to center of bearings, equal to 66.0 feet. The girders are AASHTO Type III girders spaced 5 feet 6 inches on center. The total width of the structure out to out of the curbs is 34 feet 4 inches. The bridge is on a 46 degree right skew. The concrete quality for the precast girders was specified to be 5000 psi at 28 days. The cast-in-place deck was specified to be 6 inches thick and to have a concrete quality equal to 4000 psi at 28 days. Transverse intermediate diaphragms 8 inches by 19 inches are located at the third points of the span. In addition, end diaphragms 10 inches by 30 inches are located at the ends of the spans. The specific girder selected for instrumentation was the second girder from the south side of the structure in span number one. The elevation view of this bridge is presented in Figure 1 and a typical cross section through this bridge is presented in Figure 2. Two cross sections were selected on this girder for the installation of strain transducers.

The selection of the cross sections to receive strain transducers was based on the following criteria. The first cross section was to be located close to the end of the girder in the region of relatively high shear, yet not so close

to the end of the girder that the end-block, the diaphragm, and the reaction would adversely affect the strain field.

Consideration was also given to embedded steel. A Pachometer was used to scan the candidate cross section locations in order to locate steel that was close to the surface and which may have affected strain readings. The first cross section was selected about 12 feet from the west end of the girder and the second cross section was selected about 29 feet 6 inches from the same end of the girder (Span length equal to 66 feet).

2.3 Installation of Strain Gages.

The surface preparation for the transducer installation was begun on July 10, and the transducer installation was completed on August 7, 1990. The procedures followed throughout the preparation phase and the installation phase were those recommended by Measurements Group Inc. of Raleigh, N.C., the supplier of all supplies and materials used for this installation.

The preparation of the surface included the scrubbing of the surface with a mild detergent followed by the drying of the surface with a warm air stream. The surface was then filled using Measurement Groups AE10 adhesive. Following this, the surface was degreased and abraded until the concrete began to be reexposed. At this point the transducer installation was begun.

The strain transducers selected for this project were Measurement group's gage number EA-06-20 CBW-120 Option W. This is the gage type recommended for installation on concrete surfaces. The gage length for these transducers is 2 inches. They were installed using the same AE10 adhesive that was used to fill the surface of the concrete. A frame constructed of steel angles was mounted on the girder at the gage installation location. This was

used to provide the required clamping pressure during the epoxy glue's curing period.

At a particular cross section the gages were located as presented in Figure 6. As can be seen by referring to the figure, a total of six rosette patterns were installed at a cross section. The rosettes were positioned so that they were opposite each other at the same elevation on the girder. There were a total of three rosettes at a cross section. A typical rosette pattern is given in Figure 7. A single longitudinal gage was mounted on the bottom center line of the girder. This layout scheme resulted in 19 strain transducers at each of two locations for a total of 38 transducers.

In order to eliminate temperature affects in the lead wires, a three wire lead system was used. In addition, to prevent errors due to different lengths of lead wires to a given rosette, all leads to a given rosette had the same length. In fact, only two different lengths of lead wire were used: 28 feet and 41 feet. One length was used to connect to cross section one, which was about at the quarter point of the span, and the longer length was used to connect to cross section two, which was about at the mid-point of the span. All lead wires to a cross section were bundled in a single cable. The two cables used were brought to a common point near the west end of the bridge. The gages were covered and protected as required of a permanent installation.

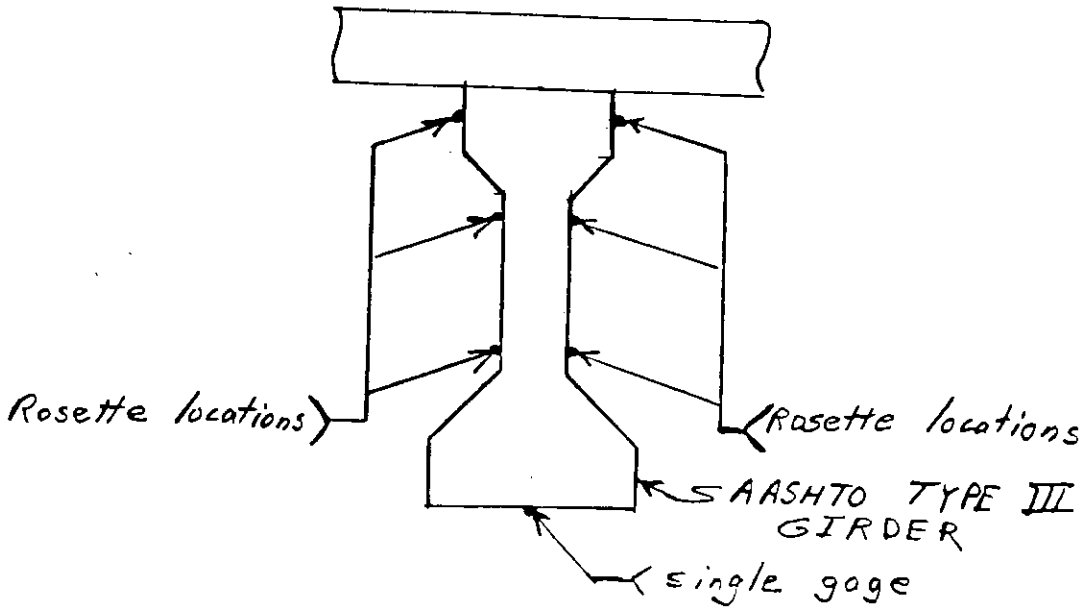

Figure 6. Typical Gage Locations

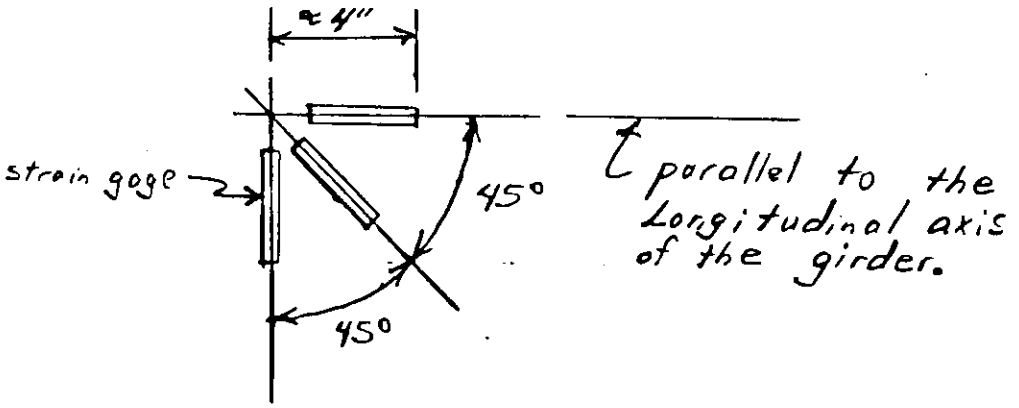

Figure 7. Typical Rosette Pattern

2.4 The Field Load Test.

In preparation for the field load test the centerline of the instrumented girder was transferred and marked on the top deck of the bridge. Four positions were marked along this alignment. These positions are detailed in Figure 8. The four positions were referred to as positions P1 through P4 with position one being closest to the west end of the structure. The axle geometry for the test truck is also given in Figure 8.

Two truck alignments were utilized during the load test. The first alignment, described as straddle (str.), centered the truck over the instrumented girder. The second alignment, described as centered (ctr.), positioned the right side set of wheels directly over the instrumented girder. The truck used for the load test was a standard tandem axle gravel truck (SDDOT truck no. DL578). The details of the truck geometry for this truck are presented in Figure 9. The truck was positioned on the structure empty, about half loaded, and fully loaded. The truck was weighed at the local SDDOT Highway Patrol Office located in Sioux Falls. The details of the truck axle weights used during the test are given in Table 2. Signing for traffic control during the test was provided by Sioux Falls personnel of the SDDOT. To define the truck position on the structure one needs to refer to one of four positions along the girder (P1 through P4) and to define the truck axle that is positioned at that location. Truck axles are be referred to by number. Axle number one is the front axle of the truck. Axle number three is the most rear axle of the tandem. The direction of the truck was such that the truck encountered positions one to four, in order, as it crossed the bridge.

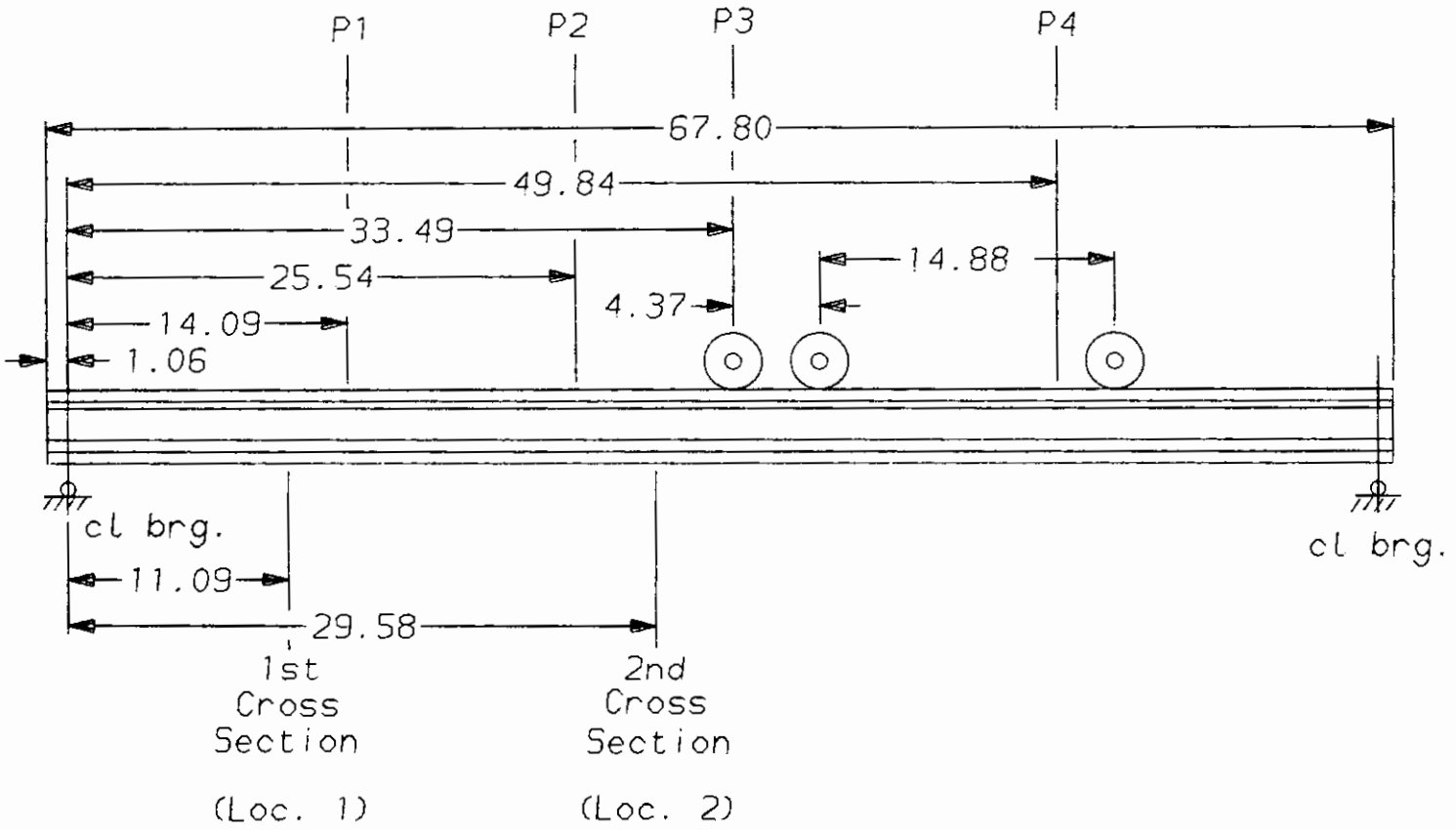

Figure 8: Long View of Girder Detailing Load Positions. (All Dimensions in Feet.)

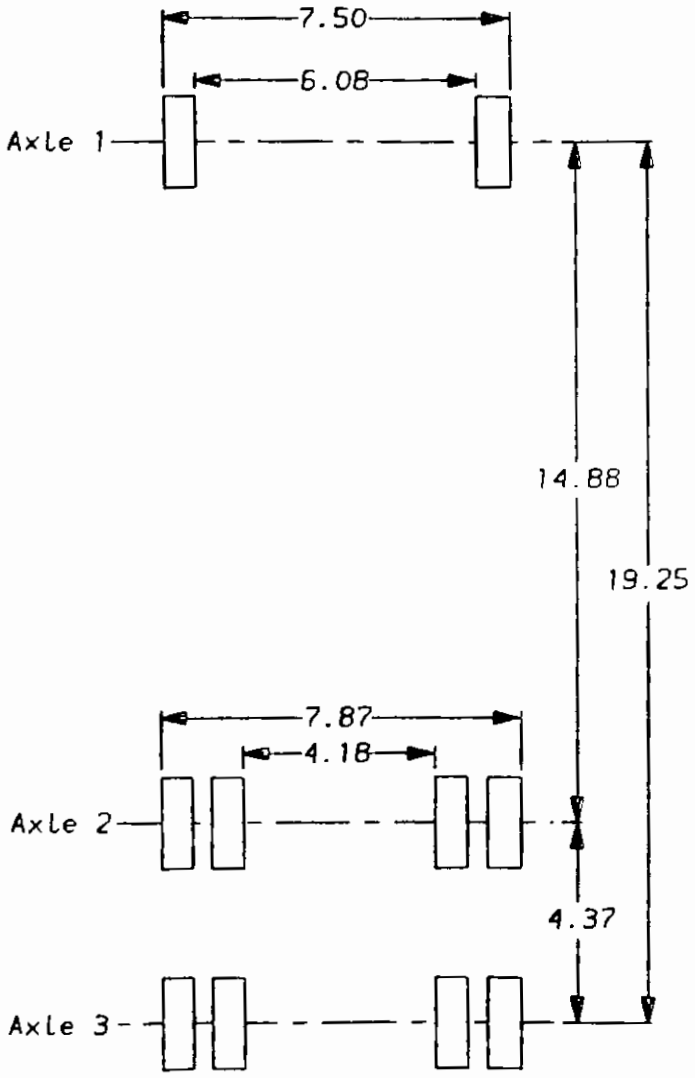

Figure 9: Test Truck Geometry
(All Dimensions in Feet.)

Table 2. Load Test Truck Weight Information*

Load	Front Axle (lbs)	Tandem Rear Axle (lbs)	Total Weight (lbs)
Empty	9,760	13,280	23,040
1/2 Load	11,420	24,560	35,980
Full Load	12,840	33,580	46,420

*SDDOT Truck No. DL578

The first load position placed axle number three at girder position one. The second load position corresponded to axle number two at girder position number two. The third load position placed axle number three at girder position number three. For the last position, the rear tandem axle was centered at girder location number four. This completed one alignment. The truck was then repositioned along the second alignment and this sequence was repeated.

At each truck position 39 transducer readings were taken. In total over 900 strain transducer readings were taken. These readings were taken using a Measurements Group Model P3500 Portable Strain Indicator. This was used in combination with four Measurements Group Model SB-10 switch and balance units. Utilizing an LVDT, deflection measurements at each truck position were taken near mid-span. To provide input voltage to the LVDT, two 12 volt lead-acid batteries were connected in series. A voltage regulating circuit was constructed that kept the input voltage at a constant level. After an initial warm-up period, the circuit input voltage was constant at 23.97 volts. The output and input to the LVDT circuit was monitored using a Fluke digital multimeter model 87. The Fluke model 87 meter has a 4 1/2 digit display. A total of 24 deflection readings were taken.

Though temperature compensating gages were used, temperatures were recorded using temperature probes at three locations adjacent to the strain transducers. These readings served as a general check on the temperature changes that occurred at the gaging locations.

The date of the load test was August 16. The first readings were taken about 8:30 a.m. and the work was completed about 2:00 p.m.. As previously stated, over 900 strain transducer readings and a total of 24 deflection readings were taken. A copy of the data taken during the test is provided in the Appendix.

2.5 Reduction of the Load Test Data.

Though temperature compensating gages were used, it was still necessary to correct the strain transducer readings for temperature. Due to the suns heating, the bridge exhibited a slow but steady tendency to camber upward from early morning to midafternoon.

Clock time and initial transducer readings were recorded at the start of each alignment sequence. After the alignment sequence was concluded the truck was driven off the structure, and the clock time and an initial set of readings were again taken. This procedure was repeated for all alignments. The individual readings were then linearly adjusted to compensate for the effect of camber.

The deflection readings were similarly treated. An initial reading was taken prior to positioning the truck. The readings were taken at each of the four positions. As above, after an alignment was completed the truck was driven off the span and another set of initial readings were taken. This permitted the linear adjustment of the individual readings. In this way the thermal camber effects were removed from the data.

The net output from each transducer was obtained by subtracting an adjusted initial reading, obtained as has been discussed, from the observed output from that specific transducer. A set of the net strains thus obtained is provided in the Appendix.

2.6 Evaluation of Inspection Data.

The objective of the inspection program was to determine the significant factors that are contributing to the observed cracking. After completion of the inspections, the data were reviewed and the descriptive adjectives used to describe the cracking were tabulated and ranked. Each was then given an arbitrary numerical rating. The result of this work is presented in Table 3. A fine crack was judged by measurement using a crack gage template to be 0.003 to 0.005 inches in width. A medium crack was determined to be about 0.010 inches in width.

Table 3. Crack Description Ratings

Rating	Crack Description	Rating	Crack Description
0	No Crack Visible	7	Minor
1	Hairline	8	Minor, Cont.
2	Hairline, Almost Cont.	8	Fine, Cont.
3	Hairline, Cont.	8	Very Noticeable, Cont.
4	Very, Very Fine	9	Significant
4	Very Fine	9	Almost Medium
5	Very Fine, Almost Cont.	10	Significant, Cont.
6	Very Fine, Cont.	10	Almost Medium Cont.
6	Almost Fine, Cont.	11	Medium
6	More Than Hairline, Cont.	12	Medium, Cont.
7	Fine		

Inspection of a typical bridge resulted in excess of 30 separate observations. An observation being descriptions taken at one side of a girder. From these separate readings, an average numerical rating was obtained for each girder, and from the girder data a single value for a bridge. The bridges, rank ordered by severity number are given in Table 4. This table lists, in addition to the severity number, whether the bridge is skewed, the year constructed, and the average daily traffic (ADT) volume.

Table 4. Average Crack Rating by Bridge

Bridge Number	Skew	Year Built	ADT	Average Crack Rating
50-173-235	Y	1981	195	0.0
50-125-168	N	1986	1400	0.3
50-310-093	Y	1964	1065	1.1
20-061-271	N	1973	1940	1.2
06-185-190	N	1966	92	1.8
51-065-050	N	1966	69	2.6
50-200-233	Y	1959	7500	3.2
50-201-233	Y	1959	7500	4.2
50-211-230	Y	1959	5565	4.3
50-210-230	Y	1959	5565	4.8
50-189-163	Y	1961	5165	6.1
50-189-164	Y	1961	5165	6.2
50-221-170	N	1961	100	6.3
50-219-210	N	1959	3370	8.9

The Computer Model.

3.1 Determining the Geometry.

In order to develop a computer model to augment the measured stresses, it is necessary to obtain information about the geometry of the bridge. In addition, it is necessary to determine estimates for the material properties of the materials in the structure, and last of all, a suitable mathematical model must be developed that will provide suitable results without overtaxing the available computing machinery. A set of Design plans were obtained from the SDDOT for the instrumented structure. One advantage of the instrumented bridge is that it is a simply supported structure. This required that only one span of the structure be modeled.

The design set of plans yielded information relative to span length, bridge width, curb geometry, girder spacing, and slab thickness. In addition the sheets held references concerning concrete strengths, prestressing information, and the quality of steel used in the project.

The selected bridge consisted of three 66 foot simple spans. The bridge has a skew of 43 degrees 57 minutes. The bridge is 34 feet 4 inches out to out of curbs. The roadway is 30 feet 0 inches from inside of curb to inside of curb. Six AASHTO Type III girders are spaced 5 feet 6 inches across the width of the bridge. A composite deck 6 inches thick was specified. A typical cross section and elevation view were previously given in Figures 1 and 2. Figure 3 contains a cross section of a typical AASHTO Type III girder. By using a level rod and an engineer's level, the deck thickness was estimated at the instrumented locations. The slab thickness that resulted from these measurements indicated that the constructed slab was very close to the design thickness. A slab

thickness of 6.0 inches was selected for use in developing the computer model. Check measurements were taken in the field of span length, bridge width, and girder spacing. All of these measurements were in very close agreement with the design specified values, therefore, the design values were used in developing the computer model.

3.2 Material Property Estimates.

The developing of material property information required more engineering judgment. Since the bridge is a composite bridge, the deck concrete is of different quality than the prestressed girder concrete. The original design called for 4000 psi concrete for the deck, and 5000 psi concrete for the prestressed girder. It is well known that concrete compressive strength increases with age. The bridge was built in 1961 so in order to estimate the concrete strength the following approach was taken.

Using a Schmidt Hammer (No. 7051), a total of 81 impact readings were taken on the girder and 50 readings were taken on the underside of the deck. From these values and the chart supplied with the Schmidt Hammer, a compressive strength of 8800 psi was estimated for the girder, and a strength of 6600 psi was estimated for the deck. The ratio of these values is 1.33. This ratio agrees favorably with the ratio of 1.25 which results from dividing the specified compressive strengths.

During the summer of 1988 several bridges in the Sioux Falls area were cored by the SDDOT. The results of 12 cores on a normal weight concrete that also had a specified compressive strength of 4000 psi was 6500 psi[1]. These bridges were built in 1958. This data gives general verification of the values

obtained from the Schmidt Hammer results. The girder compressive strength was selected as 8800 psi and the slab compressive strength was selected as 6600 psi.

After an estimate of the compressive strength was obtained, the next step was the selection of the modulus of elasticity. The formula in the American Concrete Institute (ACI 318-83) was not used to determine the modulus of elasticity. Instead, a recent formula[2] developed at Cornell University for high strength concrete was used. This formula is:

$$E_c = (40{,}000 \quad f'_c + 1{,}000{,}000)(W_c/145)^{1.5}.$$

This formula is recommended for normal weight concretes having compressive strengths (f'_c) ranging from 3000 to 9000 psi. The W_c term is the unit weight of the concrete. This was assumed to be 148 lbs./ft^3 . This formula resulted in a modulus of elasticity of 4,900,000 psi for the girder and a value of 4,380,000 psi for the slab. For the girder this formula yields a value 12 percent less than the ACI formula, and for the slab the formula yields a value 9 percent less than the ACI formula. An additional consideration is the modular ratio E_{slab}/E_{girder}. The ratio using the Cornell formula is 0.894, the ratio using the ACI formula is 0.867, a difference of 3 percent.

An estimate also must be made for Poisson's ratio. Poisson's ratio varies from 0.15 to 0.22[3]. A value of 0.15 was selected. A sensitivity study was carried out to see what effect a difference in the Poisson's ratio had on the calculated result. Changing Poisson's ratio from 0.15 to 0.20 changed the maximum deflection about 0.4 percent and the maximum observed moment about 3 percent. Therefore, the calculated results are relatively insensitive to the specific value of Poisson's ration used.

3.3 Model Selection and Development.

All modeling work was carried out on the Prime Computer System located in the Engineering College's Computer Aided Design Laboratory. The software used was the ANSYS Software Package version 4.4.

After several different finite element models were tried, a grid finite element model was selected to model the bridge. The bridge was modeled in the longitudinal direction with composite girders having the cross section of a typical composite girder. Transverse to the length of the girder, slab beam elements were employed. The bridge contains end and intermediate diaphragms, these were included in the model. A typical mesh layout is presented in Figure 10.

A computer model was developed for each truck position. This resulted in a total of eight computer models. Each model required about 550 degrees of freedom to complete its description. Besides the eight truck positions, a zero-skew computer model was developed. For this case, the same model was used as for a skewed structure except that the skew was eliminated. The objective of the computer model was to compute moment, shear, and torsional moment at intervals along the span. The selected sections for computing forces included the instrumented cross sections. In addition, the deflection was computed at the location on the span at which the deflection readings were taken.

All these data were used to help evaluate the performance of the test structure against the design model. That is to answer the question- is the structure performing essentially as the designer expected, or because of the cracking is the performance of the structure detrimentally affected.

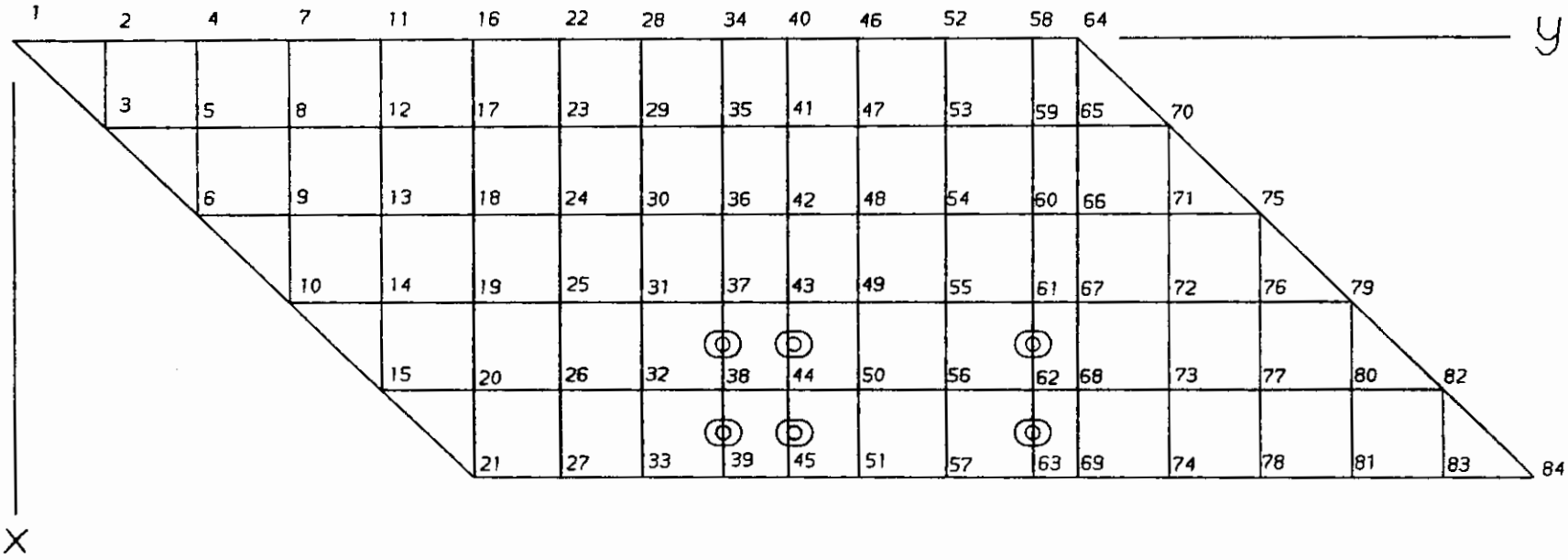

Figure 10. Typical Finite Element Mesh for the Instrumented Structure.

4.0 Results.

4.1 Observations from the Bridge Inspections.

The following observations characterizing the cracking are provided as the result of the visual inspection of the bridges. The observed cracks were in some cases very short and intermittent. In other instances they were continuous over several feet. In some cases they appear on one side of the web and then not on the opposite side of the web. If the crack is continuous for several feet it will be observed on both sides of the web. It is not unusual to observe a similar crack in the web portion of the girder just above the bottom chamfer of the cross section. These lower cracks are never as well developed as those on the top section of the web.

As the inspections progressed, it seemed to the author, that traffic density was a significant factor in determining the extent of the observed cracking. This seemed so, because the more extensive (longer continuous cracks) cracks seemed to occur on bridges that were carrying higher traffic densities. Some of the cracks appear to be initially caused by plastic shrinkage[3,4]. In this case the plastic shrinkage crack appears as a wider crack. Frequently, a hair line crack extends from this crack for several inches.

It also appeared that the differential shrinkage within the cross section, that occurs as the concrete cures, is a possible factor[3,4]. As the concrete begins to cure, the effects of gravity will cause the concrete to settle. The concrete in the top section of the 'I' shaped cross section may 'hang up', while the lower section settles slightly. This relative settlement will result in a tendency to cause a void at the base of the top chamfer of the 'I' shaped cross section. A second factor that may also contribute to a tendency

to cause a weakness at this location, is the differential shrinkage of the concrete that takes place as the concrete takes its final set. It can be expected that due to the application of heat to accelerate the cure, and even without heat, thinner portions of the cross section cure more rapidly than thicker portions. This results in differential shrinkage strains within the profile of the cross section. The form causes restraint that contributes to the tendency to cause cracking. These factors may cause cracks in the cross section, or may result in a weaker zone of concrete at the upper and lower portions of the straight section of the web which corresponds to the locations at which the cracking is observed.

4.2 Statistical Results From the Inspections.

As has already been described, the subjective visual inspection data that had been taken was transformed into numerical data that permitted the application of statistical techniques to evaluate the probable cause of the observed cracking. The bridges, ranked according to crack rating, have been presented in Table 4. The methods that were used in the analysis are those methods that have been developed for application to small samples. Each of the methods used, employ setting up a joint distribution based on the hypothesis that is being tested. A statistic applicable to the test being performed is then calculated. This calculated statistic is compared to a table value for this specific statistical test. The hypothesis is then either accepted or rejected at the checked confidence level based on the compared values.

Hypothesis no. 1: The age of the structure is related to the crack development.

In order to test this hypothesis, four statistical tests were applied: Fischer's Exact Test, The Kolmogorov-Smirnov test, The Mann Whitney Test, and

Kendall's Test. The full details will not be discussed but the general nature of the tests will be given as well as the result of the tests.

In order to perform the Fischer's exact test the sample population must be divided into two approximately equal groups according to age, and into two approximately equal groups according to the crack severity number. This test was inconclusive, that is, based on this test one could neither accept or reject the suggested hypothesis.

The Kolmogorov test was also applied to this hypothesis. To perform this test, the sample is divided into approximately two equal groups according to age. The other argument in this statistic is crack severity. This was divided into four approximately equal ranges. Less than two, between two and four, between four and six, and the last group being greater than six. The result of this test indicated that with 99 percent confidence one may accept the hypothesis, that is, the age of the bridge is related to the crack severity rating.

The Mann-Whitney Test is a test that is applicable to small samples with one rankable category which is the situation that we have. The sample is categorized exactly the same as in the Kolmogorov-Smirnoff test. This test is considered to be more accurate for small samples. The result of this test indicated with 99 percent confidence that the hypothesis may be accepted.

A fourth test that can be applied is Kendall's Test. This test requires two ranked categories. The crack severity number was grouped as for the Kolmogorov-Smirnoff test, i.e. less than two, two to four, four to six and greater than six. The age was divided into less than thirteen years, thirteen to twenty-six years, and greater than twenty-six years. Working with the table

thus defined, this test leads to the conclusion that the hypothesis may be accepted at the 99 percent confidence level.

These results lead to the adoption of the stated hypothesis that bridge age is related to crack severity.

Hypothesis No. 2: The crack severity number is related to cycles of loading.

A scaled value of cycles was used for computation. The scaled number used was computed as the Average Daily Traffic (ADT) times the age in years of the bridge. To compute the Fischer's Exact Test the bridges were grouped into two groups with crack severity less than 4, and into two groups according to whether the cycles were more or less than 100,000. This test was again inconclusive.

To compute the Kolmogorov-Smirnoff test, the crack severity range was divided as previously stated (Four categories: <2, 2-4, 4-6, >6). The cycles range was divided at the 100,000 cycles value. This test leads to the result that the hypothesis may be accepted at the 95 percent confidence level. The Mann-Whitney Test was conducted on the same table arrangement as for the Kolmogorov-Smirnoff Test. The result was that the hypothesis may be accepted at the 99 percent confidence level.

To perform Kendall's Test, the crack severity scale was divided as for the previous two tests. In addition, the cycles scale was divided into four ranges. The first range included bridges with less than 10,000 cycles (Note that a scaled value of cycles is being used.), the second range extended from 10,0000 to 100,000 cycles, the third range extended from 100,000 cycles to 200,000 cycles, and the last range included structures with scaled cycle values greater than 200,000 cycles. This analysis yielded the result that the hypothesis may

be accepted at the 98 percent confidence level. These results substantiate the hypothesis that the crack severity number is related to the cycles of loading.

Linear regression techniques were next applied to the data. In linear regression one has an argument, x and a table of values that are considered to be f(x) or values of y. Linear regression techniques find the best straight line fit for the data. Four schemes were applied: first, x any y were assumed to be linearly related; second, the logarithm of x was related to y; third, the logarithm of y was related to linear x; fourth, the logarithm of x was related to the logarithm of y.

Based on hypothesis #1 (Crack severity number vs. age), the best correlation was obtained assuming both age and the crack severity number were linear. This yielded a correlation coefficient of 0.91. The next best correlation coefficient was obtained assuming that the crack severity number was linear and age was logarithmic. This yielded a correlation coefficient of 0.88.

Based on Hypothesis no. 2 (Crack severity number vs. cycles of loading), the best correlation coefficient was obtained assuming that the crack severity number was linear and the cycles were logarithmic. This yielded a correlation coefficient equal to 0.86. The next closest result was obtained assuming both crack severity number was linear and the age was linear. This yielded a correlation coefficient equal to 0.78.

Hypothesis No. 3: Bridge skew is related to the crack severity.

To perform the Kolmogorov-Smirnoff test the crack severity scale was divided as before, that is, less than 2, 2 to 4, 4 to 6, and greater than 6. The bridges were divided into two groups skewed and unskewed. The statistic was computed and it was determined that there was no basis for accepting the

hypothesis. The Mann-Whitney test also led to the conclusion that there was no basis for accepting the hypothesis.

In order to perform Kendall's Test the crack severity scale was divided as in the preceding paragraph. The skew was grouped as either zero skew, skew less than or equal to 27 degrees, and a third group was defined representing skews greater than 27 degrees. The test statistic was computed with the result that there is no statistical basis for accepting the hypothesis. All three tests gave no basis for selecting the hypothesis that skew is related to the crack severity.

The conclusions reached testing hypotheses numbers 1 and 2 are significant, but the problem is that both age and cycles of loading are likely to be somewhat correlated. This is the case because one obtains cycles of loading by applying a multiplier to the ADT that is directly correlated to time. To offset this problem somewhat it was decided to test hypothesis no. 4.

Hypothesis No. 4: Average daily traffic (ADT) is related to crack severity.

To compute the Fischer's Exact Test the crack severity scale was divided into two segments. The scale was split at a crack severity number equal to 4. The ADT scale was divided into two segments at the ADT value of 4000. The results of this test indicated that the results were significant at the 91 percent confidence level.

To compute the Kolmogorov-Smirnoff test the crack severity range was divided as has been previously stated (Four categories: <2, 2-4, 4-6, >6). The ADT scale was divided as stated for the Fischer's Exact Test. This test leads to the result that the hypothesis may be accepted at the 95 percent confidence level.

The Mann-Whitney test and Kendall's test were conducted on the same table as for the K-S test. The results from these two tests indicate that the hypothesis may be accepted at the 95 percent confidence level for the Mann-Whitney test and at the 98 percent confidence level for Kendall's test. These results lead to the acceptance of the hypothesis that average daily traffic (ADT) is related to the crack severity.

Hypothesis No. 5: Deck replacement is a significant factor in contributing to the cracking.

Deck replacement was looked at as a factor in the cracking. No conclusive results could be obtained concerning this hypothesis. An attempt was made, but it must be noted that the sample that can be used to test this hypothesis is very small. Only four bridges of those inspected had deck replacement; and these four were older bridges, all built in the same year. The remaining older bridges were used as a comparison group. The problem is that the group is too small to draw conclusions. The tests did not show any statistical basis for accepting the hypothesis that crack severity was related to deck replacement.

In summary it is noted that five hypotheses were tested using the inspection data. These were: No. 1, Bridge ageing is related to Crack Development; No. 2, The crack severity number is related to cycles of loading; No. 3, Bridge skew is related to the crack severity; No. 4, Average daily traffic (ADT) is related to crack severity; and No. 5, Deck replacement is a significant factor in contributing to the cracking. Four statistical tests that are applicable to small samples were applied. These were the Fischer's Exact Test, The Kolmogorov-Smirnoff Test, The Mann-Whitney Test, and Kendall's Test. These tests indicate that based on the results of the inspections, ageing load cycles

and average daily traffic are significant factors contributing to the cracking. The skew is not statistically significant as contributing to the cracking. It was not possible to separate age and load cycles so they must be accepted as a combined effect. The sample size was too small to statistically evaluate whether deck replacement was a factor. Barring unbalanced girder loads during deck replacement, it is the author's opinion that deck replacement is not a significant factor contributing to the cracking.

4.3 Strain Measurements and Computer Model Results.

As has been stated, the bridge was modeled in the longitudinal direction with composite girders having the cross section properties calculated under the assumption of composite behavior. Transverse to the length, wide beam elements were employed. The truck was positioned on the computer model corresponding to the truck positions used on the instrumented bridge. The truck positions on the span and the geometry of the truck were previously presented in Figures 8 and 9.

In presenting and discussing the results, the following notation has been employed. The locations at which the strain readings have been taken are referred to as 'Loc.1' for location 1 and 'Loc. 2' for location 2. The truck positions are referenced as 'P1', position 1; 'P2', position 2; 'P3', position 3; and 'P4' as position 4. The two alignments are referred to as 'str.' or 'ctr.'. The 'str.' notation refers to the situation in which the truck was centered on the instrumented girder. The dual wheels in this case straddled the instrumented girder. The other alignment notation used is 'ctr.'. In this case, the right hand set of wheels was centered over the instrumented girder. The truck positions and instrumented cross section locations may be reviewed by referring to Figure 8.

4.4 Comparison of Flexural Strains and Measured Strains.

Moments were obtained from the computer model corresponding to the locations at which the instrumention was located. From the moments, stresses were calculated on the bottom fiber of the girder. These stress values were then converted to strain readings. For the fully loaded truck these values are compared to the field observed readings and are presented in Table 5.

By consulting this table, it is noted that the model values are with one exception, greater than the measured strains. Though some percent differences are large, the absolute differences in the microstrain readings are not very large. If one concentrates on the larger readings, i.e. readings greater than 20 microstrain, it is observed that the average difference between the observed reading and the model value is -13.0 percent. If one subtracts the microstrain values for these same larger readings, and averages the difference, it is -4.0 microstrain. The fact, that with one exception all observed readings are less than those obtained from the model, indicates that the actual structure is stiffer than the computer model. This is an indication that the structure is not losing stiffness due to the cracking. These values are considered to represent very good correlation between theory and the measured values.

4.5 Evaluation of the Measured and Model Deflections.

A total of eight computer models were developed. This number corresponds to the four truck positions on the two alignments. The wheels of the fully loaded truck were positioned on each model according to the truck geometry previously given in Figure 9. Since a linear model was used the deflections for the partially loaded truck were obtained by proportion.

Table 5. Summary of Maximum Flexural Stresses and Strains. Fully Loaded Truck

Truck Position	Location 1 (approximately 1/4 pt.)					Location 2 (Near Midspan)				
	Moment (in-lbs)	Model Stress (psi)	Model Strain E	Meas. Strain E	% diff.	Moment (in-lbs)	Model Stress (psi)	Model Strain E	Meas. Strain E	% diff.
Str, P1	1,080,000	114.3	23.3	19	-18.4	1,351,000	143.0	29.2	26	-11
Str, P2	691,200	73.1	14.9	12	-19.5	1,698,000	179.7	36.7	32.5	-11
Str, P3	309,700	32.8	6.7	7	+ 4.4	1,528,000	161.6	33.0	32.5	-1.5
Str, P4	109,600	11.6	2.4	2	-16.7	581,500	61.5	12.6	8	-36
Ctr, P1	1,203,000	127.3	26.0	22	-15.4	1,310,000	138.6	28.3	23.6	-16.7
Ctr, P2	890,700	94.2	19.2	12	-37.5	1,620,000	171.4	35.0	29.2	-16.6
Ctr, P3	379,700	40.2	8.2	4	-51.0	1,362,000	144.1	29.4	23.8	-19.0
Ctr, P4	127,070	13.4	2.7	1	-63.0	+ 440,100	46.6	9.5	9.4	-1.0

The results from the model and the observed deflections are presented in Table 6. In addition Figures 11 and 12 present both theoretical and observed load vs. deflection lines for all alignments and truck positions.

Initially comments will be directed to the numbers in Table 6. Of the 24 observed values, 19 are less than the values obtained from the computer model. This is about 80 percent of the values. The range in the differences is from -36.4 percent to +8.8 percent. Both of these extremes being achieved on the empty truck at small measured deflections. Ignoring the sign, the average difference is 7.4 percent.

If one restricts ones attention to observed values greater than 0.0300 inches (This value, 0.0300 inches, is 44 percent of the maximum observed deflection of 0.0675 inches.), the following comments can be made. The average absolute difference is 4.9 percent with 76 percent of the 17 values being negative. A negative difference indicates that the computer model deflection was more than the observed deflection on the instrumented structure.

The specific comments stated above can be observed qualitatively by referring to Figures 11 and 12. Very good linearity is noted in the observations presented in the figures. Again, the analysis supports the theory that the actual structure is exhibiting a stiffness greater than the stiffness exhibited by the computer model.

Shear effects are not reflected in the computed values in Table 6. These effects were not considered significant. In order to check this assumption, a separate analysis was conducted with the truck centered (Ctr.) in position 2 (P2). The maximum deflection for the model that included shear effects was 0.6 percent more than the value which did not include shear effects.

Table 6. Summary of Deflections

Truck Position	Truck Empty (23,040) Theor (in)	Meas (in)	% Diff.	Truck 1/2 Full (35,980) Theor (in)	Meas (in)	% Diff.	Truck Full (46,420) Theor (in)	Meas (in)	% Diff.
Str, P1	0.0297	0.0323	+ 8.8	0.0464	0.0459	-1.1	0.0599	0.0566	-5.5
Str, P2	0.0349	0.0366	+ 4.9	0.0546	0.0543	-0.5	0.0704	0.0675	-4.1
Str, P3	0.0335	0.0328	- 2.1	0.0522	0.0520	-0.5	0.0674	0.0666	-1.2
Str, P4	0.0179	0.0168	- 6.1	0.0280	0.0302	+7.8	0.0361	0.0384	+6.4
Ctr, P1	0.0292	0.0261	-10.6	0.0456	0.0437	-4.2	0.0588	0.0546	-7.1
Ctr, P2	0.0339	0.0291	-14.1	0.0529	0.0486	-8.1	0.0682	0.0626	-8.2
Ctr, P3	0.0300	0.0246	-18.0	0.0468	0.0432	-7.7	0.0604	0.0575	-4.8
Ctr, P4	0.0143	0.0091	-36.4	0.0223	0.0202	-9.4	0.0288	0.0289	+0.3

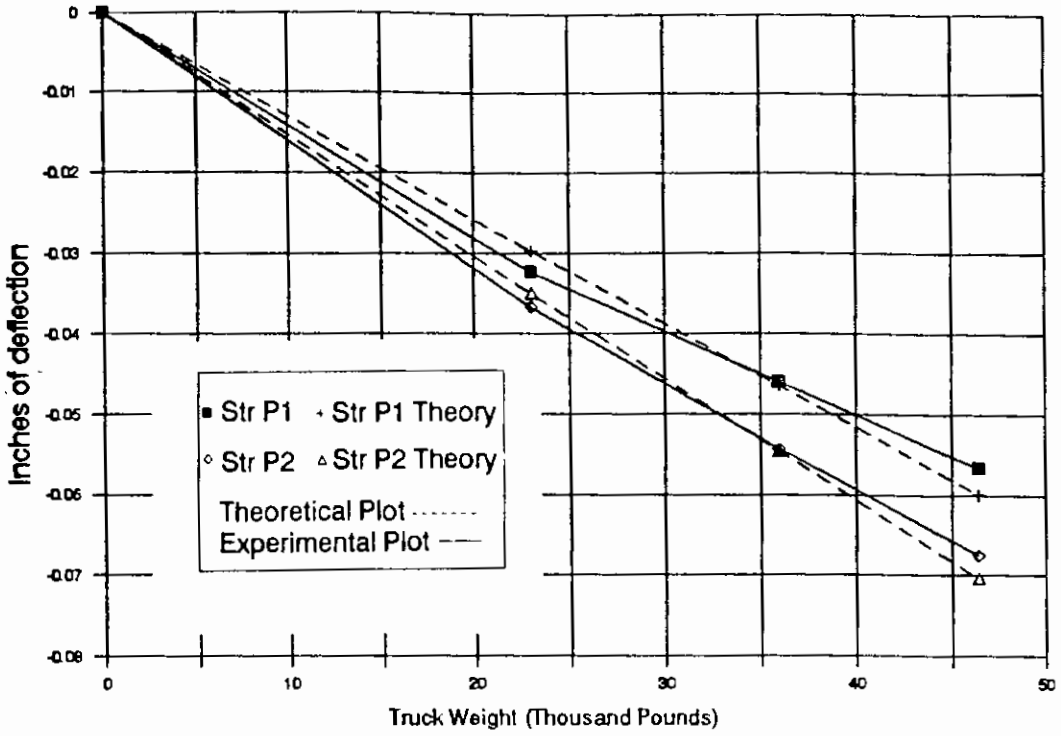

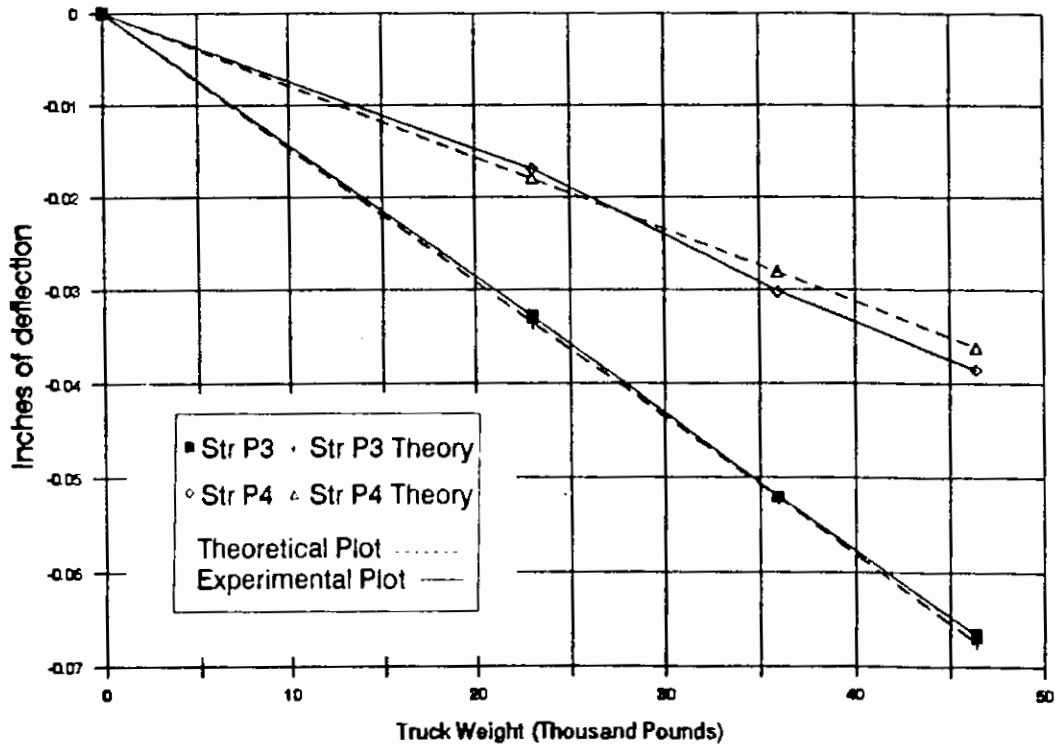

Figure: 11
Truck Weight vs Deflection
Straddle Alignment, all truck positions

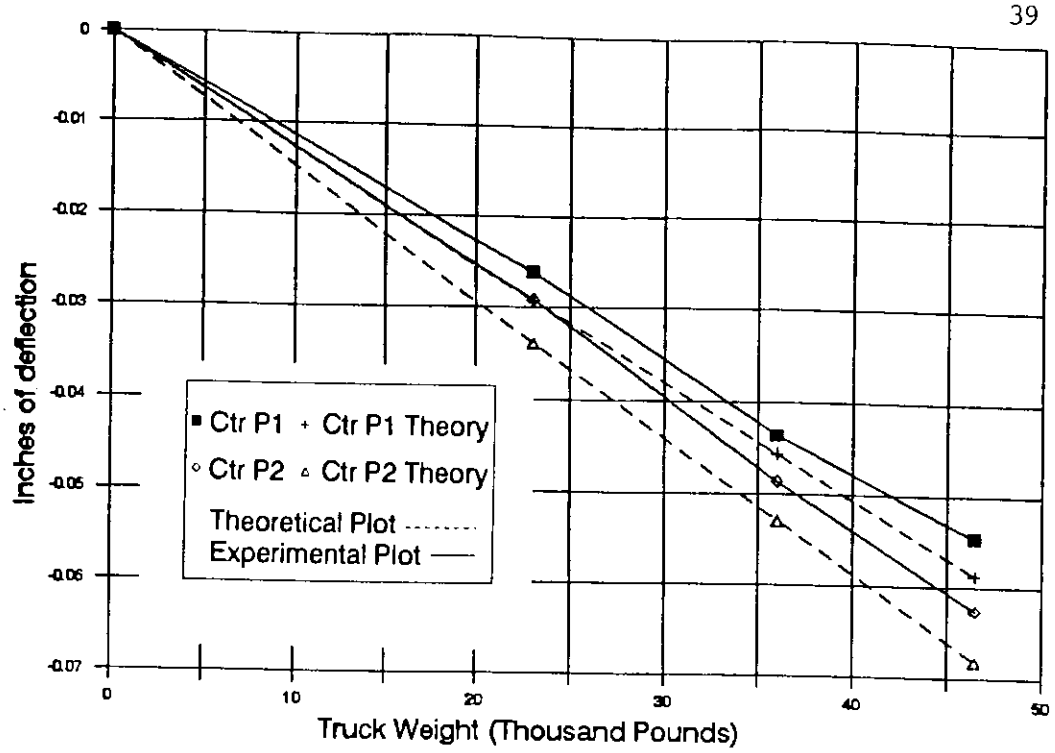

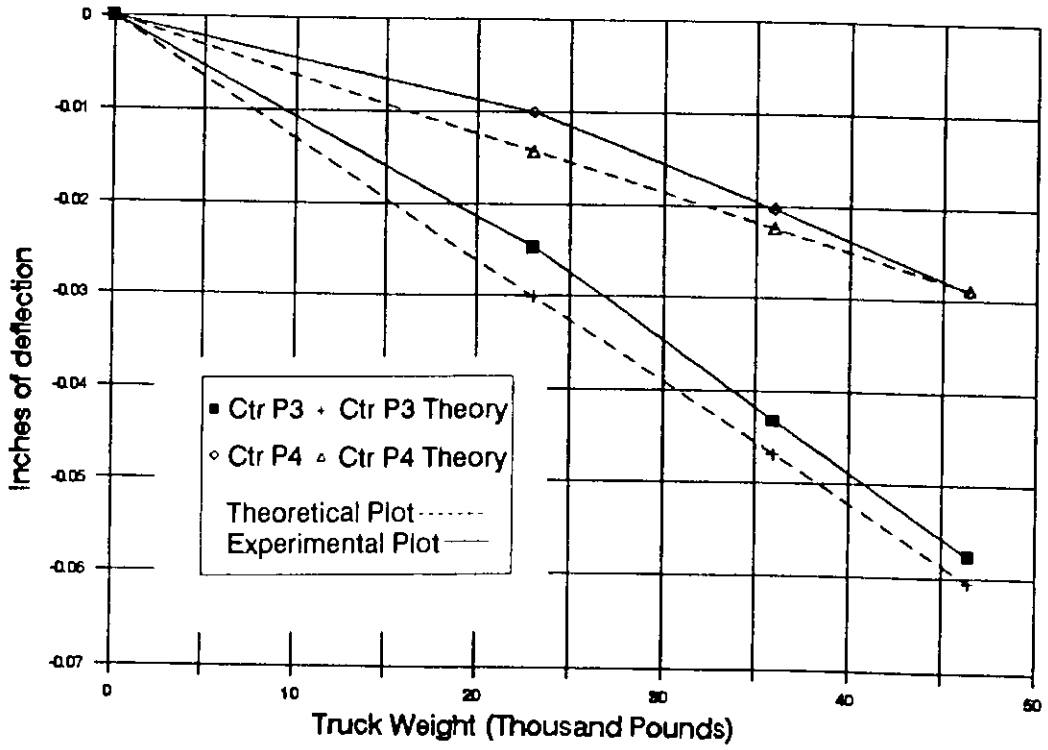

Figure: 12
Truck Weight vs Deflection
Centered Alignment, all truck positions

The moments increased only about 0.2 percent as compared to the moments that did not include the shear effects. From this it can be observed that the shear effects do not significantly affect the computed results.

4.6 Cross Section Neutral Axis Location Investigation.

The strain readings on the horizontal gages were used to estimate the location of the composite neutral axis on the cross section. Be referring to the previously presented Figures 6 and 7, it can be observed that there were a total of 7 gages available at an instrumented cross section that can be used to estimate the location of the neutral axis. The reason the neutral axis location is significant, is that if the cracks are affecting the integrity of the cross section the neutral axis will shift. This can be observed by using the strain transducer readings to locate the neutral axis and by comparing these values with the theoretical location computed under the assumption of composite behavior.

Each truck position resulted in a set of readings at each instrumented cross section. These readings can be used to estimate the location of the neutral axis. Three different truck weights were used and for each truck weight, the truck was positioned in eight different locations. This resulted in 24 different estimates of the neutral axis location at each intrumented cross section.

Regression techniques were used to estimate the neutral axis location. The traditional least squares technique was used along with a technique that minimizes the horizontal distance from the estimated line to the measured strain readings. The results of these calculations are presented in Table 7. The neutral axis locations given in the table are given in inches from the bottom surface of the cross section. As can be seen in the table the theoretical

Table 7. Summary of Neutral Axis Locations.
(All units inches)

	Location 1		Location 2		Average Both Locations	
	Least Squares	Least Horiz.	Least Squares	Least Horiz.	Least Squares	Least Horiz.
Average	33.93	30.84	32.29	31.98	33.09	31.41
Std. Dev.	5.8	3.8	2.4	2.0	4.5	3.1
Theory	31.0	31.0	31.0	31.0	31.0	31.0
Difference	2.9	-0.2	1.3	1.0	2.0	0.4

Table 8. Confidence Limits on the Neutral Axis Location (inches)

Conf. Inter.		Location 1 Least Squares	Location 1 Least Horiz.	Location 2 Least Squares	Location 2 Least Horiz.	Average Both Locations Least Squares	Average Both Locations Least Horiz.
95%	Upper	36.3	32.4	33.2	32.8	34.4	32.2
	Lower	31.6	29.3	31.3	31.2	31.8	30.5
	Diff.	4.7	3.0	1.9	1.6	2.6	1.8
98%	Upper	36.7	32.6	33.4	32.9	34.6	32.4
	Lower	31.1	29.0	31.1	31.0	31.6	30.4
	Diff.	5.6	3.6	2.3	1.9	3.0	2.1

location is 31 inches from the bottom surface of the beam. Confidence limits of 95 percent and 98 percent are given in Table 8.

A representative set of the results from the strain transducers are presented in Figures 13 and 14. Combined on theses graphs are the least square regression lines, and the theoretical strain line based on the stresses obtained from the computer model. To preserve clarity, only the full truck and empty truck results are presented on these graphs.

Inspecting Table 8 reveals that the worst deviation from theory is 2.9 inches at location one. This location is approximately at the quarter point of the span. Results at location 2 which is near the center of the span deviate by only about 1.0 inch. By inspecting Table 8 it is seen that the theoretical value of 31 inches lies just outside the lower 95 percent confidence limit for the least squares technique. The theoretical value lies within the 95 percent confidence limit for the least horizontal distance technique.

These results are considered to demonstrate good agreement between the theoretical location of the neutral axis and the measured neutral axis location in the actual structure. In addition the measured strains are considered to demonstrate good linear behavior through the depth of the cross section. The greatest deviation from the 31.0 inch value occurs at the lower load levels when the strain values are small, i.e. in the range of 4 or 5. It must be pointed out that measuring strains on concrete is itself subject to variation simply due to the presence of aggregate particles of various sizes which may affect the strain field in close proximity to the strain transducer.

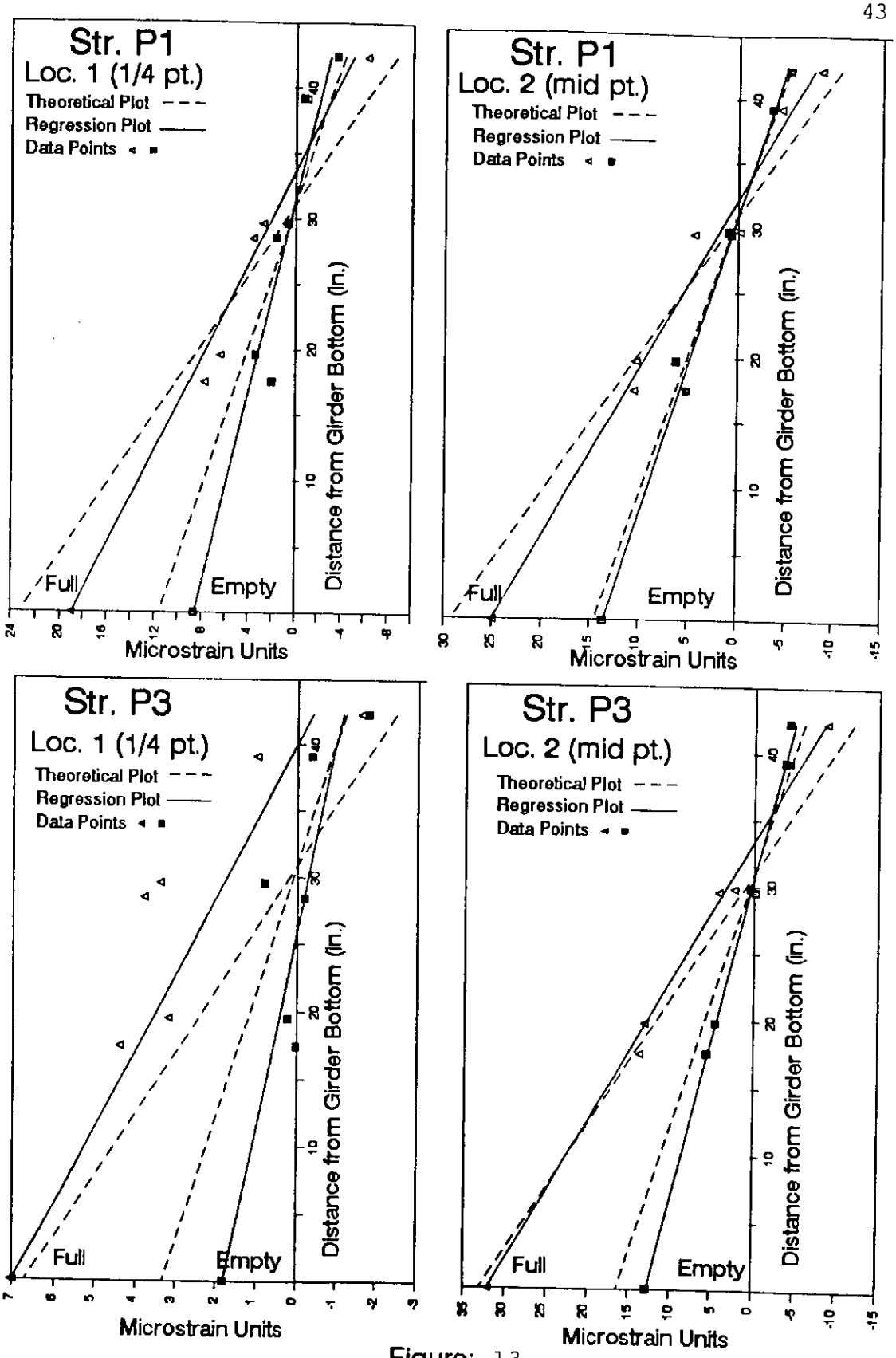

Figure: 13

Strain vs Distance from the bottom fiber of the beam
Straddle Alignment, Positions P1 and P3

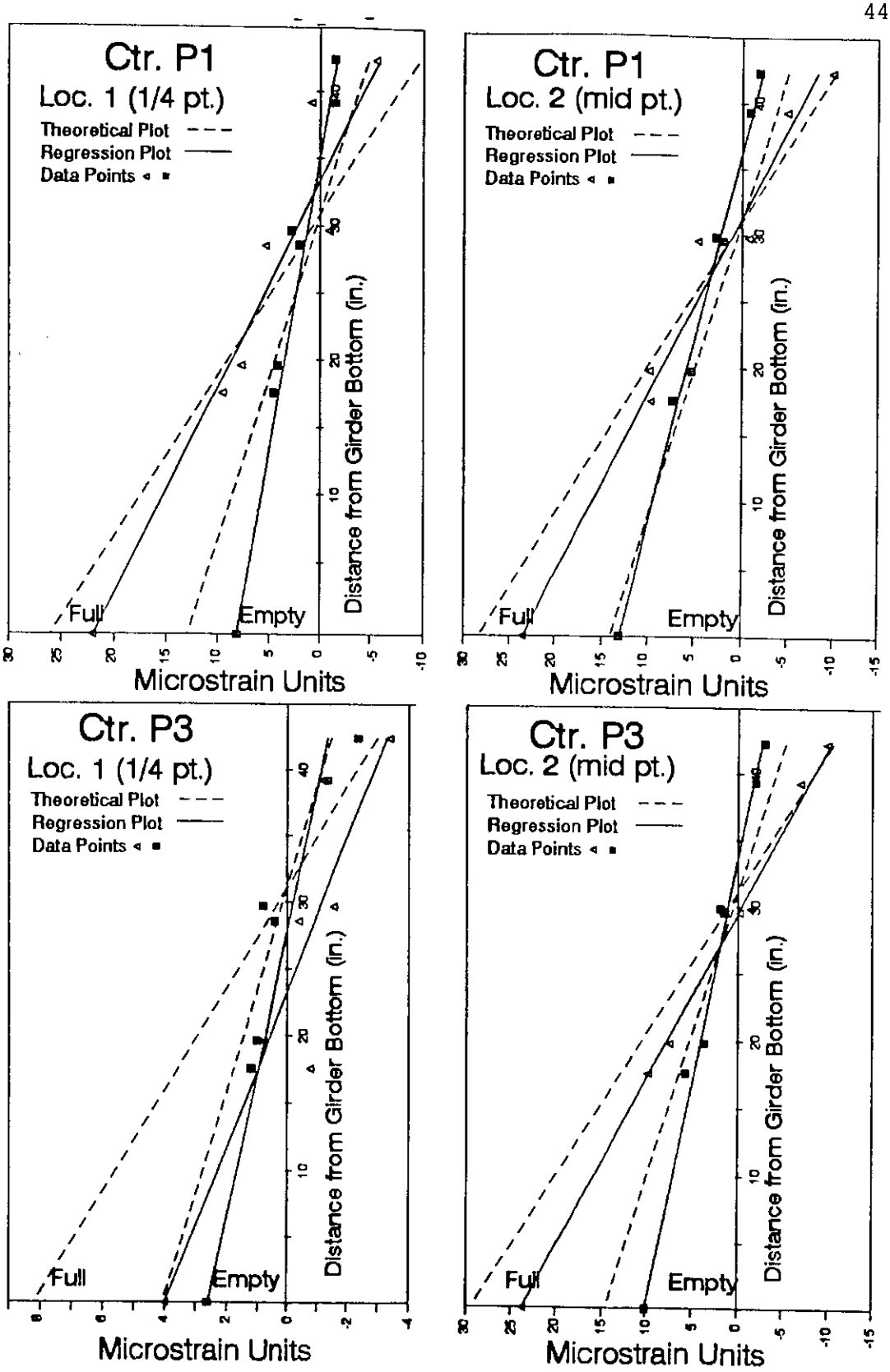

Figure: 14

Strain vs Distance from the bottom fiber of the beam
Centered Alignment, Positions P1 and P3

4.7 Torsion and Shear Analysis of the Cross Section.

In the process of performing the computer modeling, it was noted that the truck that was used to perform the load test generated torsional moments that were on the order of 6 to 10 percent of the live load moment. These values are not considered large, but an analysis was performed in order to determine the adequacy of the cross section for this torsional moment. In order to assess the significance of these forces, a dead load analysis had to be performed. It was found from the dead load analysis that the structure is subjected to dead load torsional moments on the order of 6 percent of the dead load bending moment. The maximum live load moment produced by the loaded test truck resulted in a maximum live load moment about 1/3 the dead load moment. This gives a perspective on the magnitudes of the moments achieved during the load test.

Since a torsional analysis is essentially a shear analysis, the shear forces had to be considered simultaneously with the torsion in order to determine the significance of these values. The theory that was employed to perform this analysis was the Skew Bending Theory that is presented in several textbooks. Representative of which are references 6, 7, and 8 at the end of this report. The details of this rather lengthy analysis will not be presented.

The conclusion of this analysis is that the shear reinforcement provided appears to be adequate to carry the combined effects of shear and torsion. The statement "appears to, " is used because no attempt was made to perform an analysis against design loads. The reinforcement provided in the girder is more than adequate to carry the loads investigated; that is, due to dead load effects plus the shears and torsional moments induced by the test truck.

4.8 Comparison of Skew vs. Zero Skew Bridge Configurations.

Because skew was considered a possible contributing factor to the cracking, a decision was made to perform a comparison analysis on a zero skew span in order to help evaluate the significance of skew on the cracking. A computer model of a zero skew span was developed. Both a dead load and live load analysis were performed on this zero skew span. The truck position selected for this analysis was the centered alignment (ctr.), position two (P2). This corresponds to the situation in which the right hand set of wheels are centered over the instrumented girder. This alignment tended to maximize the effect of torsion on the skewed bridge and also developed a close to maximum bending moment. Truck position 2 can be noted by referring to Figure 8.

A summary of the results from this analysis is presented in Table 9. It is observed that the dead load shear, bending moment, and deflection, are significantly increased in the zero skewed bridge when compared to the skewed configuration. The torsion in the girder is significantly decreased when compared to the skewed span. It is interesting to note that the truck associated live load shear, bending moment, and deflection are not significantly increased in the zero skew bridge. The truck induced live load torsional moment was reduced in the zero skew span about 40 percent as compared to the same value in the skewed bridge. This compares to a reduction of about two thirds for the dead load torsion. This result demonstrates that the torsion is significantly less in a zero skew span as compared to a skewed span.

It is interesting to note that the truck induced live load moment is approximately the same in the unskewed span as compared to a skewed span. In the author's opinion this gives general confirmation to the result obtained from the statistical analysis that there is no significant difference in the cracking

Table 9. Analysis Results from the Skew vs. Zero Skew Span Analysis.

	Shear (kips)	Torsion (kip-in.)	Bending Mom. (kip-in.)	Defl. (in.)
Skew (D.L.)	32.0	379.5	5,790	.267
Z.Skew (D.L.)	43.8	124.0	8,610	.407
Per. Dif.	+36.6	-68.0	+48.0	+52.0
Skew (L.L.)	7.2	107.2	1,910	0.068
Z.Skew (L.L.)	8.1	61.8	1,925	0.072
Per.Diff.	+11.8	-42.3	+0.5	+5.9

D.L. signifies dead load values.
L.L. signifies live load values.

observed in the skewed and unskewed spans. Since the live load effects are similar in the skewed and unskewed structure it is expected that the two structures will demonstrate similar cracking. Though it does not prove fatigue is a factor, it demonstrates that the stress ranges observed in the skewed vs. non skewed bridges will be of similar magnitude. Since stress range along with cycles of loading are significant fatigue considerations; it adds additional credibility to the theory that fatigue is a significant factor.

5.0 Summary of Results.

The statistical analysis of the inspection data provided the following results. The hypothesis that the age of a bridge is related to the severity of the observed cracking proved significant at the 99 percent confidence level in

three of the four tests used to evaluate this hypothesis. In addition, the age of the bridge was observed to exhibit a linear correlation coefficient of 0.91 when compared to the assigned crack severity number. This indicates that age is a factor in contributing to increased cracking.

The hypothesis that cycles of loading are significant in contributing to the crack severity proved to be an acceptable hypothesis at equal to or greater than the 98 percent confidence level in three of the four tests used to evaluate this hypothesis. A regression technique utilizing the crack severity number and the logarithm of the cycles of loading yielded a correlation coefficient of 0.86. This indicates that cycles of loading are significant in causing increased cracking.

The hypothesis that average daily traffic (ADT) is significant in contributing to the cracking proved significant at the 95 percent confidence level in all of the tests used except the Fischer's exact test which indicated the hypothesis is significant at the 91 percent confidence level. This indicates that ADT is significant in promoting the cracking.

Because of the small sample size, it is not possible to separate age and cycles of loading as separate significant factors. With the result obtained from the ADT analysis, there is a strong suggestion that the live load stress ranges experienced by a structure due to traffic contribute to the cracking and age alone is not a primary factor.

The hypothesis that the bridge skew is a significant factor in causing the cracking could not be accepted by any of the tests performed. The sample for testing whether deck replacement was a significant factor was so small that no conclusions could be reached. It seems logical that deck replacement by itself,

barring unforeseen construction loads that occur during the deck replacement, should not be a significant factor in promoting the cracking.

The results from the comparisons of the measured bottom fiber flexural strains and the values obtained from the computer model indicate that with one exception all the measured values are less than the values obtained from the computer model. If one examines the larger readings, i.e. values greater than 20 microstrain, one observes that the average difference between the measured and the calculated values is a minus 13 percent. The range in the differences over these same larger readings ranges from -19 percent to -1.5 percent. The minus signs indicating that the measured values average less than the analytical values. This is considered very good correlation between measured and calculated values. It is noted that a 10 percent difference with respect to a 20 microstrain value is only 2 microstrain and these results are from measurements on concrete.

Twenty-four observations of deflection were made during the load test. When these readings are compared to deflections obtained from the detailed computer model of the structure about 80 percent of the observed readings are less than the computed values. If one concentrates on the 17 observed deflections larger than 0.030 inches (The largest observed deflection was 0.0675 inches.), the average absolute difference is 4.9 percent with 76 percent of these larger values being less than the corresponding analytical value. The range in the differences between the observed and analytical values for these 17 values is -8.2 to +8.8 percent. These results demonstrate very good agreement between the observed and computer calculated results. These results also demonstrate that the actual structure is exhibiting a stiffness greater than the computer model.

The flexural strain readings were used to evaluate the location of the neutral axis on the cross section. The assumption being that if the cracking were causing a deterioration in the integrity of the cross section; the flexural strains will be affected, and the neutral axis will show a shift away from the theoretical design assumed location. Two regression techniques, the familiar least squares method and a technique that minimizes the horizontal distances to the data points, were used to obtain 24 estimates of the neutral axis locations at each of the two instrumented cross sections.

The least squares technique yielded a neutral axis location of 33.1 inches from the bottom surface of the beam. This value is the average of both instrumented cross sections. The standard deviation on this value is 4.5 inches. The 95 percent confidence limits on the average produces a range from 31.8 inches to 34.4 inches. The theoretical location is estimated to be 31.0 inches from the bottom surface of the girder. This is observed to lie just outside the 95 percent confidence limits.

The least horizontal distance regression technique yielded a comparative neutral axis location of 31.4 inches. The standard deviation on this value is 3.1 inches. The 95 percent confidence limits on the average produces a range from 30.5 inches to 32.2 inches. In this case the theoretical value of 31.0 inches is observed to fall near the center of the interval.

These two methods are considered to substantiate the conclusion that the neutral axis location has not moved, and thus, the results add validity to the conclusion that the integrity of the cross section is not affected by the cracking. The fact that one method locates the neutral axis just outside the confidence interval and the second at the center of the confidence interval is not considered contradictory. The girder spacing (five feet six inches.) is

reasonably close in this bridge. The instrumented girder is the second girder from the outside of the bridge. At the edge of the bridge is a substantial curb element that will affect the neutral axis location on the instrumented girder. It can be shown that if one takes the three outside girders and includes the curb element, the neutral axis for these three girders will be located 33.2 inches (Compares to 33.1 inches by least squares and 31.4 inches from the least horizontal dimension technique.) above the bottom of the cross section.

From the results of the torsion and shear analysis, the girder appears to be adequately designed to carry the shear and torsion introduced in the skewed bridge. The analysis on the zero skew span didn't produce any unusual information. The only point that emerged is the known fact that a skewed span has significantly greater torsional effects as compared to zero skew span. The interesting point is that the live load effects due to the truck are not significantly different in the skewed vs. the zero skew configuration. This shows that live load stress ranges will be comparable in the two configurations. This also substantiates the conclusion from the statistical analysis that skew by itself is not a significant factor in the cracking.

As a closing comment to the results summary, the author points out that due to the differential shrinkage of the cast in place deck shear stresses are introduced into the prestressed girder. These can be rather significant depending upon the assumptions that are made, though the developing creep strains will tend to reduce these effects with time. These shrinkage induced shear stresses are not considered by themselves to be a significant factor, but they are considered to be contributory to the development of a stress situation that promotes cracking.

6.0 Conclusions.

The project had the following objectives:

1. To determine the probable cause of the cracking.
2. To determine if the presence of the cracking has reduced the strength of the girder.
3. To determine if epoxy injection will effectively repair the girders.

Based on the results obtained during this study the following conclusions have been reached.

1. Both age and cycles of loading are significant factors in producing the cracking that was observed in the structure.
2. Average daily traffic (ADT) and thus loadings caused by traffic are significant in contributing to the cracking.
3. The skew of the bridge is not by itself a significant factor in causing the cracking.
4. The presence or absence of deck replacement is not considered to be a significant factor in the cracking.
5. Based on the agreement between the measured and calculated stresses and deflections, the structures do not appear to be detrimentally affected by the cracking.
6. Based on the analysis of the measured flexural strains, the integrity of the cross section has not been detrimentally affected by the presence of the cracking.

7.0 Comments and Recommendations.

It is the opinion of the writer that the observed cracking is contributed to by two factors. The first factor is the volume change that takes place in the concrete girder during its initial curing period. These volume changes are those associated with plastic shrinkage, and differential shrinkage due to the differing hydration rates portions of the cross section experience. It is believed that in some cases these effects cause cracks to form at the base

of the chamfer on the top portion of the 'I' section and also along the top portion of the bottom chamfer of the 'I'. It is probable that even in cases in which the cracks are not formed, a weak zone is formed in some of the girders at these locations. Subsequently, with the combined effects of differential shrinkage of the composite deck and the application of live loads, a shear crack forms and then slowly propagates along the web. It is believed that once the crack forms it takes very little stress to cause it to advance.

The second factor is the live load shear stresses imposed by the traffic. The shear stresses cause diagonal tension stresses that either result in the formation of the crack due to the presence of tensile shrinkage strains, or extend the crack if the crack is already present. Shear stresses are considered significant because of where the cracks are located. The neutral axis of the cross section is located almost exactly at the location of the cracks. The flexural stresses are essentially zero at this location; therefore, they cannot be contributing to the cracking. As is known from basic flexural theory, the shear stresses are maximum at the neutral axis, and these shear stresses produce diagonal tension stresses. It is these tensile stresses that contribute to the propagation of the cracks.

Stresses must be contributing to the cracking because the statistical analysis identified cycles of loading, average daily traffic, and age as significant factors contributing to the cracking. Load cycles are directly stress related, and average daily traffic (ADT) also points to stress as a contributing factor. Age alone is a puzzling factor. It could simply be a chance factor because cycles of loading accumulate with time, or it may indicate that the fabrication practices have improved with the result that newer girders do not develop volumetric effects that contribute to the cracking.

Since shear stresses are stated as contributing to the cracking it may be asked, why are the cracks horizontal rather than at the expected 45 degree angle? It is true that in reinforced concrete beams shear cracks are oriented at a nearly 45 degree angle relative to the longitudinal axis of the member, but in prestressed concrete beams because of the significant axial compressive stress in the member the diagonal tension cracks are oriented at a much shallower angle. This will be explained by making use of Figure 15. In Figure 15 a) and b) are sketched two simple beams. Figure 15 a) illustrates a reinforced concrete beam with a section cut showing the internal forces acting on the cross section. In Figure 15 b) is shown a similar figure for a prestressed member. The internal forces are similar in the two figures except in the case of the prestressed member there is a significant axial compressive force due to the prestress effect.

In Figure 15 c) and d) are shown the stresses on differential elements taken at the neutral axes of the members. These figures are also similar except that there is no normal stress on the element taken from the reinforced concrete member. This is because the differential element was taken at the neutral axis of the member, and the flexural stress which is the only contributor to the normal stress is zero at the netural axis. There is a normal stress on the differential element taken from the prestressed member because of the axial prestress force applied to the member. Also presented at the lower right in Figures 15 c) and d) are the maximum principal stresses resulting from the analysis of the stresses at this point in the member. Discussion of these elements will be delayed following the discussion of the Mohr's circle analysis in Figures 15 e) and f).

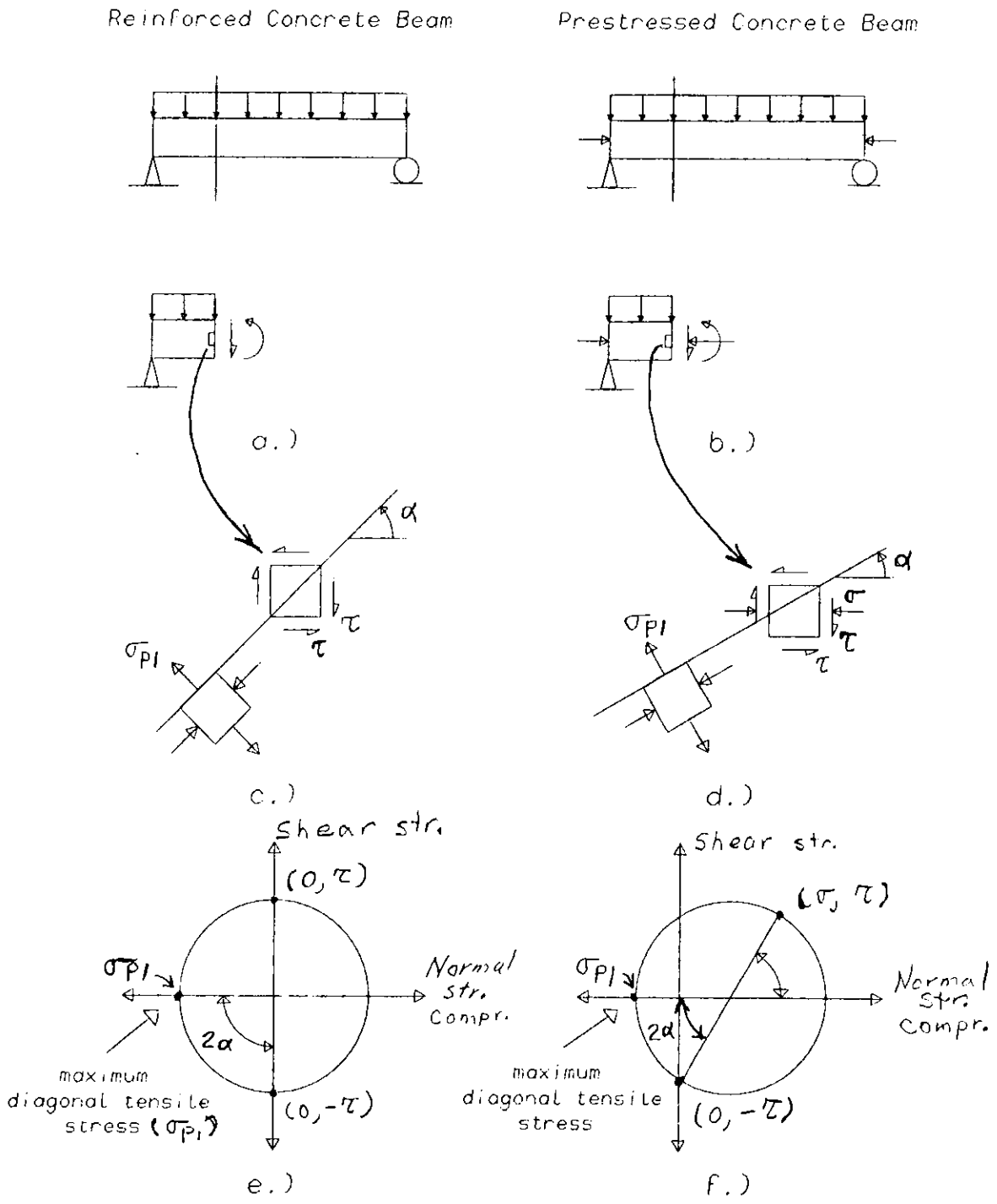

Figure 15: Shear Stress Analysis of Reinforced Concrete Beam and Prestressed Concrete Beam.

In Figures 15 e) and f) are shown the Mohr's circles for the stresses acting on the elements. In Figure 15 e) is the analysis for the reinforced concrete member. The maximum principal tensile stress is located 90 degrees on the Mohr's circle which represents a 45 degree orientation on the actual element (On the Mohr's circle all angles are double). Since the angle is 45 degrees from the horizontal and if the tensile stresses are sufficient to crack the concrete, the resulting diagonal tension crack will be oriented at a 45 degree angle perpendicular to the actual direction of principal tensile stress. In the case of the prestressed member the angle (α) between the horizontal axis of the member and the plane of maximum principal tensile stress is much less than 45 degrees. This results in a diagonal tension crack being oriented at a relatively shallow angle to the horizontal axis of the member. These different angular orientations can be seen by referring back to Figures 15 c) and d).

This analysis points out two major differences in the effect of shear stresses on reinforced concrete and prestressed concrete beams. The first, which has already been pointed out, is that diagonal tension cracks, when they form, are oriented at a shallow angle to the longitudinal axis of the member. The second difference is that because of the longitudinal compressive stress it will take a greater shear stress to cause a diagonal tension crack. This is offset though because one uses prestress members in longer spans which has the effect of increasing shear stresses.

Because the cracks appear at the neutral axis of the member where the flexural stresses are zero, and because cycles of loading and ADT have proved significant in causing the cracking, for these reasons the shear stresses caused by the vehicle traffic are considered to be a significant cause in promoting the cracking. The fact that the cracks trend along the horizontal are considered to

be explained by the immediately previous discussion which details the shear effects in prestressed concrete beams.

It should be noted that all the cracks observed were very small. A fine crack being about 0.005 inches and a medium crack about 0.010 inches wide. If one does not know what to look for, one can easily miss the cracks that were listed as hairline. In general, none of these cracks appear to represent a significant threat to the service life of the girder; though not much is known about prestressed concrete members under cyclic live load shear stresses. The studies the author consulted concentrated on fatigue in flexure. The phenomenon under study is believed to result from shear stresses.

One objective of this study was to determine whether epoxy injection would be effective in remedying the cracking. The author is not experienced with epoxy compounds and the comments that follow were obtained from reference nine listed at the end of this report. Since the cracks are very fine, injection techniques are the methods that are likely to have the best chance for success. In many of the bridges inspected, the cracking is not sufficiently extensive to justify trying to seal the cracks with epoxy. Cracks as narrow as 0.002 inches have been successfully sealed using epoxy injection techniques[4]. If the crack is active, and this is considered to be the case since the cracking is attributed to live load stresses, the crack is likely to reappear after the injection grouting technique is applied[4]. The cracking is not considered detrimental since the shear reinforcement is considered adequate to carry the imposed stresses.

The main consideration should be the prevention of in-migration of moisture which will cause the onset of corrosion. It is noted that the girders, particularly the interior girders, are in a relatively protected environment due to the presence of the overhead slab. Nevertheless, it was observed during the

inspections that in a few instances corrosion was occurring on the shear reinforcement.

No results from this study indicate that the capacities of the affected girders are significantly reduced due to cracking. Therefore, there is no reason that the girders cannot be reused if a deck replacement is planned for a particular bridge. In situations in which deck replacement is going to be undertaken, care should be observed during the deck removal phase of the project in order to minimize unbalanced loading that will cause bending about the longitudinal axis of the girder. It is the writers opinion that the more significant cracking that occurred during the deck replacement on the Sioux Falls 18th Street bridge was due to the presence of existing cracks and the unbalanced loading due to the construction techniques used.

REFERENCES

1. Sigl, Arden B., "The Umbrella Bridge Project," Final Report, Contracting Agency: South Dakota Department of Transportation, Jan. 1989.

2. Carrasquillo, R.L., Nilson, A.H., and Slate, F.O., "Short Term Mechanical Properties of High Strength Concrete Subject to Short Term Loads.", J.ACI, Vol. 78, No. 3, May-June 1981 pp. 171-178.

3. "Finite Element Analysis of Reinforced Concrete", Task Committee on Finite Element Analysis of Reinforced Concrete Strcutures of the Structural Division Committee on Concrete and Masonry Structures, American Society of Civil Engineers, 1982," p. 36.

4. "Causes, Evaluation, and Repair of Cracks in Concrete Structures," Report by ACI Committee 224, American Concrete Institute, Report no. ACI 224.1R-84, 1984.

5. "Control of Cracking in Concrete Structures," Report by Committee 224, American Concrete Institute, Report no. ACI 224R-80, 1985.

6. Hsu, Thomas T.C., Torsion of Reinforced Concrete, Van Nostrand Reinhold Co., 1984, pp. 171-202.

7. Nilson, Arthur H., Design of Prestressed Concrete, 2nd ed., John Wiley and Sons, 1987, pp. 234-250.

8. Nawy, Edward G., Prestressed Concrete, Prentice Hall, 1989, pp. 253-305.

9. "Use of Epoxy Compounds with Concrete," Report by Committee 503, American Concrete Institute, Report No. ACI 503R-80, 1985.

APPENDIX

1. Copy of the Data Sheets
2. Copy of the Net Strain Readings
3. Diagram Detailing Transducers Locations

APPENDIX A

Copy of the Data Sheets

All Tabulated Strain Values are in Microstrain Units.

LOAD TESTING - BRIDGE ANALYSIS PROJECT

	Start	Final
Time	8:19 am	8:59 am
Volt In.	23.98	23.97
Temp 1	64 °F	64 °F
2	63.5 °F	63.5 °F
3	61 °F	62 °F

Loading Situation:
1: West most
2:
3:
4: East most
Straddle/Cntr line/Off set

Truck: Weight-Axle Front 9760 Rear 1 Rear 2 13280 Number DL 578 Load: Empty/(1/2)/Full

Gage Number:	Initial	1	2	3	4	Final
1	746	744	746	747	749	749
2	867	866	867	868	868	866
3	866	866	865	864	864	862
4	1796	1797	1799	1796	1795	1798
5	332	329	331	332	334	332
6	956	956	956	952	960	955
7	1259	1260	1259	1256	1257	1256
8	1962	1966	1964	1961	1961	1959
9	683	684	684	683	682	681
10	623	631	629	623	621	620
11	533	530	532	533	535	536
12	532	527	528	529	531	532
13	785	786	786	784	783	781
14	-484	-483	-483	-484	-485	-486
15	-396	-389	-382	-391	-394	-396
16	181	183	183	182	183	183
17	913	910	910	911	912	912
18	1511	1512	1519	1514	1513	1511
19	1440	1442	1441	1440	1440	1440
X	142	144	146	147	148	149
21	636	633	633	634	637	639
22	675	675	695	673	674	674
23	432	430	429	428	428	427
24	-1197	-1196	-1195	-1196	-1196	-1195
25	1468	1470	1471	1467	1466	1468
26	1681	1680	1680	1680	1680	1680
27	1466	1472	1472	1470	1468	1465
28	297	298	296	350	297	296
29	-218	-220	-220	-220	-220	-220
30	2513	2526	2526	2524	2515	2510
31	1251	1246	1246	1248	1251	1253
32	1112	1107	1107	1107	1109	1111
33	541	540	539	538	537	535
34	2400	2401	2401	2401	2401	2401
35	1492	1493	1492	1496	1492	1491
36	1123	1122	1121	1120	1119	1118
37	1036	1041	1042	1041	1037	1035
38	807	803	802	806	800	797
39	2306	2304	2303	2304	2303	2302
Defl	0.4534	- 0.2885	- 0.3585	- 0.2320	0.182	0.618

1/10

LOAD TESTING - BRIDGE ANALYSIS PROJECT

	Start	Final
Time	9:15am	9:33am
Volt In	23.9	
Temp 1	64°F	
2	64°F	
3	63°F	

Loading Situation:
1: West most
2:
3:
4: East most
Straddle/(Cntr line)/Off set

Truck: Weight-Axle Front 9761 Number..... Load:
Rear 1.....
(Empty)/(1/2)/Full
Gage Rear 2 13,280
Number:

Gage Number:	Initial	1	2	3	4	Final
1		751	752	753	754	755
		865	865	864	865	865
2		859	858	857	856	856
		1779	1779	1779	1780	1781
3		328	329	332	332	334
		898	898	901	901	901
4		1259	1257	1256	1255	1255
		1926	1914	1962	1960	1960
5		683	682	682	681	680
		619	622	619	616	614
6		535	535	536	538	540
		527	527	528	529	531
7		781	779	778	778	775
		483	485	481	487	488
8		285	288	291	294	296
		125	124	124	184	184
9		908	904	907	908	908
		1518	1517	1511	1510	1508
10		1440	1442	1440	1440	1438
		153	153	154	154	156
X		639	638	640	643	640
		675	673	672	673	672
11		423	422	422	421	419
		1193	1193	1193	1193	1194
12		1469	1469	1465	1467	1467
		1675	1672	1673	1674	1674
13		1470	1469	1468	1466	1464
		296	293	296	295	294
14		223	225	225	223	223
		2522	2521	2517	2509	2505
15		1252	1251	1253	1256	1258
		1107	1107	1108	1110	1111
16		534	533	533	530	529
		2404	2403	2406	2403	2403
17		1496	1494	1498	1493	1491
		1122	1122	1122	1118	1116
18		1042	1041	1040	1029	1034
		803	801	804	798	795
19		2303	2303	2303	2301	2300
Defl		0.047	0.030	0.192	0.595	0.891

2/10

LOAD TESTING - BRIDGE ANALYSIS PROJECT

	Start	Final
Time	10:13 am	10:43 am
Volt In.	23.97	23.97
Temp 1	64.5°F	66.0°F
2	64.0°F	65.0°F
3	63.5°F	60.5°F

Loading Situation:
1: West most
2:
3:
4: East most
Straddle/Cntr line/Off set

Truck: Weight-Axle Front 11421 lb Rear 1 [illegible] Rear 2 7455 lb Number DL Load: Empty/(1/2)/Full

Gage Number:	Initial	1	2	3	4	Final
1	772	760	762	764	765	767
2	872	862	864	866	864	862
3	845	842	847	843	840	839
4	1785	1787	1787	1788	1787	1789
5	334	326	329	332	333	333
6	894	891	892	892	892	894
7	1255	1265	1259	1237	1256	1256
8	1952	1966	1962	1960	1959	1952
9	672	677	677	677	676	674
10	606	618	613	607	603	601
11	546	541	540	545	547	549
12	532	518	519	521	523	526
13	765	764	764	763	762	759
14	-491	-489	-489	-490	-491	-494
15	-295	-280	-281	-285	-290	-296
16	186	185	189	182	188	188
17	905	901	901	901	902	901
18	1506	1518	1516	1512	1509	1504
19	1428	1442	1421	1437	1438	1436
X	165	167	169	169	170	170
21	668	647	646	647	651	652
22	668	668	665	665	667	666
23	408	405	410	404	403	402
24	-1190	-1187	-1186	-1188	-1185	-1188
25	1467	1470	1473	1465	1467	1466
26	1670	1670	1670	1669	1675	1662
27	1464	1472	1474	1474	1469	1466
28	393	395	392	390	397	394
29	-226	-228	-228	-227	-227	-228
30	2498	2517	2521	2517	2503	2495
31	1265	1257	1256	1254	1264	1267
32	1110	1105	1105	1102	1107	1110
33	518	518	517	515	515	513
34	2405	2407	2408	2407	2407	2406
35	1488	1489	1487	1493	1490	1486
36	1101	1102	1106	1104	1104	1104
37	1031	1040	1042	1039	1034	1030
38	790	794	792	799	792	787
39	2294	2292	2292	2291	2292	2292
Defl	1.483	0.440	0.297	0.410	0.944	1.775

3/10

LOAD TESTING - BRIDGE ANALYSIS PROJECT

	Start	Final
Time	10:50am	11:11am
Volt In	12.97	
Temp 1	66.2°F	
2	66.0°F	
3	65.5°F	

Loading Situation:
1: West most
2:
3:
4: East most
Straddle/Cntr line/Off set

Truck: Weight-Axle Front 11420 lb Number..... Load:
Rear 1.....
Rear 2. 23560 lb
Empty/(Full)/Full

Gage Number:	Initial	1	2	3	4	Final
1		760	766	769	771	773
2		856	860	862	863	861
3		836	835	834	835	835
4		1789	1789	1790	1792	1793
5		322	325	329	322	320
6		862	862	865	862	871
7		1261	1259	1258	1258	1258
8		1948	1946	1962	1967	1965
9		677	676	677	675	674
10		615	608	602	600	599
11		544	544	549	552	553
12		519	520	523	525	527
13		762	761	760	757	756
14		-488	-488	-490	-493	-494
15		-296	-279	-283	-288	-292
16		191	191	192	192	192
17		896	897	898	900	900
18		1516	1512	1509	1507	1505
19		1402	1440	1439	1438	1438
X		173	174	174	175	175
21		650	651	652	656	659
22		668	667	664	665	665
23		399	398	399	399	398
24		-1184	-1183	-1185	-1184	-1185
25		1469	1470	1463	1466	1467
26		1661	1659	1658	1662	1664
27		1473	1474	1474	1470	1468
28		293	290	298	296	294
29		-233	-233	-233	-230	-230
30		2513	2515	2511	2498	2491
31		1260	1260	1262	1267	1269
32		1104	1106	1105	1109	1111
33		514	514	514	513	510
34		2408	2410	2410	2410	2410
35		1492	1492	1499	1493	1482
36		1110	1113	1113	1108	1105
37		1039	1041	1039	1033	1031
38		794	793	801	792	787
39		2293	2294	2295	2294	2292
Defl		0.788	0.928	0.919	1.528	2.073

1/10

LOAD TESTING - BRIDGE ANALYSIS PROJECT

	Start	Final
Time	12:45 pm	1:14 pm
Volt In.	23.98	23.98
Temp 1	70.0°F	71.0°F
2	68.0°F	69.0°F
3	69.0°F	69.3°F

Loading Situation:
1: West most
2:
3:
4: East most
Straddle/Cntr line/Off set

Truck: Weight-Axle Front 12,940 lb Number..... Load:
Rear 1. 33,560 lb
Rear 2.
Empty/(1/2)/(Full)

Gage Number:	Initial	1	2	3	4	Final
1	788	786	788	791	791	790
2	862	867	866	869	868	863
3	825	824	824	824	827	825
4	1808	1811	1812	1813	1813	1812
5	341	331	335	340	342	342
6	889	882	882	884	887	888
7	1280	1271	1270	1269	1267	1267
8	1961	1972	1969	1965	1963	1962
9	670	671	672	673	671	670
10	586	605	598	593	588	586
11	563	557	560	562	561	564
12	526	515	516	520	521	526
13	745	748	748	749	746	745
14	502	498	497	498	501	503
15	289	268	268	273	282	289
16	202	206	208	207	205	204
17	894	891	893	895	893	893
18	1503	1522	1520	1516	1509	1503
19	1441	1443	1448	1446	1442	1442
X	179	181	181	180	178	175
21	672	668	668	669	671	674
22	661	663	665	661	663	662
23	395	385	385	388	387	386
24	1175	1170	1168	1169	1171	1172
25	1472	1477	1482	1472	1473	1473
26	1663	1663	1665	1668	1665	1664
27	1973	1484	1488	1488	1480	1476
28	299	301	300	312	303	302
29	231	232	231	229	232	230
30	2481	2507	2516	2516	2493	2486
31	1278	1270	1269	1271	1273	1281
32	1115	1109	1111	1109	1110	1119
33	499	499	502	504	500	504
34	2423	2424	2427	2429	2424	2429
35	1485	1486	1486	1488	1489	1489
36	1091	1091	1092	1092	1088	1093
37	1033	1045	1051	1051	1040	1040
38	782	786	788	802	789	786
39	2283	2281	2283	2284	2283	2286
Defl	3.382	2.042	1.798	1.836	2.528	3.467

5/10

LOAD TESTING - BRIDGE ANALYSIS PROJECT

	Start	Final
Time		1:42 pm
Volt In		
Temp 1		
2		
3		

Loading Situation:
1: West most
2:
3:
4: East most
Straddle/Cntr line/Off set

Truck: Weight-Axle Front..... Number..... Load:
Rear 1..... Empty/(1/2)/Full
Gage Rear 2.....

Number:	Initial	1	2	3	4	Final
		789	789	790	792	
1		861	862	864	865	
2		826	824	825	827	
3		1815	1813	1813	1815	
4		327	329	336	340	
5		875	872	877	883	
6		1275	1271	1269	1269	
7		1976	1974	1966	1965	
8		673	672	672	671	
9		608	598	590	587	
10		558	557	560	563	
11		520	520	522	526	
12		752	751	749	749	
13		-494	-496	-499	-501	
14		-261	-266	-275	-281	
15		210	207	206	208	
16		891	889	889	892	
17		1523	1515	1510	1508	
18		1452	1447	1443	1441	
19		173	171	171	172	
X		669	666	667	673	
21		667	663	658	662	
22		388	386	386	389	
23		-1167	-1169	-1171	-1169	
24		1478	1477	1465	1471	
25		1657	1652	1651	1659	
26		1486	1486	1484	1480	
27		300	295	306	304	
28		-235	-238	-237	-231	
29		2509	2514	2508	2492	
30		1270	1268	1268	1276	
31		1110	1113	1108	1117	
32		504	505	505	507	
33		2428	2429	2427	2430	
34		1494	1493	1501	1495	
35		1099	1104	1102	1099	
36		1049	1053	1048	1044	
37		794	793	803	794	
38		2287	2288	2288	2289	
39						
Defl		2.179	2.010	2.153	2.861	

LOAD TESTING - BRIDGE ANALYSIS PROJECT

	Start	Final
Time	1.44 pm	1.58 pm
Volt In.	23.98	23.98
Temp 1	72.0 F	73.0 F
2	69.7 F	70.0 F
3	70.0 F	71.0 F

Loading Situation:
1: West most
2:
3:
4: East most
Straddle/(Cntr line)/Off set

Truck: Weight-Axle Front..... Number..... Load:
Rear 1..... Empty/(1/2)/(Full)
Rear 2.....

Gage Number:	Initial	1	2	3	4	Final
1	792		791			793
2	864		863			865
3	827		825			827
4	1816		1817			1818
5	343		331			340
6	888		875			887
7	1269		1273			1270
8	1964		1972			1964
9	670		672			670
10	586		596			584
11	513		559			565
12	528		521			528
13	748		752			748
14	-504		-496			-504
15	-287		-265			-285
16	208		209			210
17	893		887			893
18	1505		1515			1505
19	1445		1448			1445
X	171		170			172
21	674		668			676
22	662		664			663
23	389		389			390
24	-1170		-1166			-1168
25	1473		1478			1474
26	1661		1651			1661
27	1477		1487			1479
28	300		295			303
29	-232		-238			-231
30	2483		2513			2485
31	1276		1267			1278
32	1118		1113			1119
33	503		506			505
34	2428		2432			2431
35	1488		1494			1489
36	1092		1103			1091
37	1037		1052			1039
38	786		793			785
39	2284		2288			2284 → 3.815
Defl	3.576	3.639	2.160	2.172		3.71
	1:44	1:49	1:50	1.56 pm.		1.58 pm 2.06 pm
	Before initial load	After initial				

7/10

APPENDIX B

Copy of the Net Strain Readings

All Tabulated Strain Readings are in Microstrain Units.

Gage Number	Str P1 Truck Weight (pounds) 23040	35980	46420	Str P2 Truck Weight (pounds) 23040	35980	46420
1	-2.6	-3	-2.4	-1.2	-2	-0.8
2	-0.8	0	-0.2	0.4	2	3.6
3	-0.8	-1.8	-1	-0.6	-0.6	-1
4	0.6	1.2	2.2	0.2	0.4	2.4
5	-4	-7.8	-10.2	-2	-4.6	-6.4
6	-1.8	-5.4	-6.8	-2.6	-3.8	-5.6
7	3.4	4.8	6.4	2.8	3.6	4.8
8	4.4	8	10.8	2.8	5	7.6
9	1.4	0.6	1	1.8	1.2	2
10	8.6	13	19	5.2	9	12
11	-3.6	-5.6	-6.2	-2.2	-3.2	-3.4
12	-5.8	-9.6	-11	-4.6	-8.2	-10
13	1.8	0.2	3	2.6	1.4	3
14	1.4	2.6	4.2	1.8	3.2	5.4
15	9	15.2	21	8	14.4	21
16	1.6	1.6	3.6	1.2	2.2	5.2
17	-2.8	-4.2	-2.8	-2.6	-2.4	-0.6
18	7	12.4	19	6	10.8	17
19	2	4.4	7.8	1	3.8	6.6
x	0.6	1	2.8	1.2	2	3.6
21	-3.6	-3.6	-4.4	-4.2	-5.2	-4.8
22	0.2	0.4	1.8	0.4	0.8	3.6
23	-1	-1.8	-0.2	-1	-1.6	-0.4
24	0.6	2.6	4.4	1.2	3.2	5.8
25	2	3.2	4.8	3	6.4	9.6
26	-0.8	0.4	-0.2	-0.6	0.8	1.6
27	6.2	7.6	10.4	6.4	9.2	13.8
28	1.2	1.8	1.4	-0.6	-0.4	-0.2
29	-1.6	-1.6	-1.2	-1.2	-1.2	-0.4
30	13.6	19.6	25	16.2	24.2	33
31	-5.4	-8.4	-8.6	-5.8	-9.8	-10.2
32	-4.8	-5	-6.8	-4.6	-5	-5.6
33	0.2	1	-1	0.4	1	1
34	0.8	1.8	-0.2	0.6	2.6	1.6
35	1.2	1.4	0.2	0.4	-0.2	-0.6
36	0	0.8	-0.4	0	-0.4	0.2
37	5.2	9.2	10.6	6.4	11.4	15.2
38	2.8	4.6	3.2	2.6	3.2	4.4
39	-1.2	-1.6	-2.6	-1.4	-1.2	-1.2

Gage Number	Str P3 Truck Weight (pounds) 23040	35980	46420	Str P4 Truck Weight (pounds) 23040	35980	46420
1	-0.8	-1	1.8	0.6	-1	1.4
2	1.6	4	6.4	1.8	2	5.2
3	-0.4	0.6	1	0.8	-0.2	2
4	-1.2	0.6	2.6	0.4	-1.2	1.8
5	-1	-1.4	-1.6	1	-0.2	0.2
6	-2.4	-3.2	-4.4	-0.2	-2.6	-1.2
7	0.2	1.4	3.2	1.6	0.2	0.6
8	0.2	2	3.4	0.6	1	1.2
9	1.2	1.8	3	0.6	1.4	1
10	1.8	4	7	0.4	1	2
11	-1.8	-2.8	-1.6	-0.4	-1.4	-2.8
12	-3.4	-5.8	-6	-1.2	-3.4	-5
13	1.4	1.6	4	1.2	1.8	1
14	1.2	2.8	4.6	0.6	2.4	1.8
15	5	10.6	16	2	5.8	7
16	-0.2	0.8	3.8	0.4	0.4	1.4
17	-1.4	-1.6	1.6	-0.2	0.2	-0.2
18	3	7.2	13	2	4.6	6
19	0	0.2	4.4	0	1.6	1.2
x	0.8	1	3.4	0.4	1	2.2
21	-3.8	-4.8	-4.2	-1.4	-1.4	-2.6
22	-1.4	-1.8	-0.6	-0.2	0.6	1.2
23	-1	-0.4	2.4	0	-0.2	1.2
24	-0.2	0.8	4.2	-0.6	0.4	1.6
25	-1	-1.4	-0.6	0	0.8	0.2
26	-0.4	0.2	4.4	-0.2	1.6	1.2
27	4.6	8.8	13.2	2.8	3.4	4.6
28	3.6	6.4	11.2	0.8	3.2	1.6
29	-0.8	0.2	1.4	-0.4	0.6	-1.8
30	12.8	20.8	32	4.4	7.4	8
31	-4.2	-9.2	-8.8	-1.6	-2.6	-7.4
32	-4.4	-8	-8.4	-2.2	-3	-8.2
33	0.6	0	2	0.8	1	-3
34	0.4	1.4	2.4	0.2	1.2	-3.8
35	4.6	6.2	10.6	0.8	3.6	0.8
36	0	-1.6	-0.2	0	-0.8	-4.6
37	5.6	8.6	13.8	1.8	3.8	1.4
38	7.4	10.8	17.6	2.2	4.4	3.8
39	0.4	-1.8	-0.8	0.2	-0.4	-2.4

Gage Number	Ctr P1 Truck Weight (pounds) 23040	35980	46420	Ctr P2 Truck Weight (pounds) 23040	35980	46420
1	0.8	-4.2	-1.4	0.6	-3.4	-1.8
2	-0.8	-3.8	-2.2	-0.6	-1.6	-1.4
3	-1.8	-2.2	0.6	-1.6	-2.4	-1.8
4	0.4	-0.8	2.2	-0.2	-1.6	-0.6
5	-5.2	-11.2	-15.2	-4.4	-8.4	-13.4
6	-6.2	-10.4	-13	-5.4	-10.8	-16
7	4	4.6	7.6	2	2.2	3.2
8	6	9.6	13.6	4	7.2	9.2
9	2.2	3	3	1.4	2	2
10	8.2	14.8	22	4.4	8.6	12
11	-1.8	-5.8	-5.8	-2.6	-4.6	-6.6
12	-4.8	-7.2	-6.4	-4.6	-6.4	-6.8
13	1.2	3.6	6.4	0.4	3.2	4.8
14	3.4	6	9.2	1.8	6	7.4
15	11	19.2	27.6	8	15.4	22.2
16	1.8	2.2	5.2	0.6	1.4	1.4
17	-3.2	-4.8	-2	-4.4	-3.6	-4
18	7.6	11.8	19.6	4.2	7.6	11.2
19	4.4	5.6	9.4	2.8	3.2	3.8
x	2.6	2	-1.2	1.2	2	-2.4
21	-1	-4.2	-5	-3	-4.4	-8
22	1.4	2.2	5	-0.2	1.4	1
23	-2.4	-2.2	1.4	-1.8	-2.4	-1.2
24	1.8	3.4	4.6	1.6	3.8	2.2
25	1.2	2.8	5	1.4	3.6	4
26	-3.8	-6.2	-6.4	-5.6	-7.4	-10.8
27	5.2	6.6	9.8	4.4	7.2	9.6
28	0.4	-1	-1.6	-2.2	-4	-6.2
29	-2.4	-4.6	-4.6	-3.8	-4.2	-7.2
30	13	18.8	23.6	13	21.6	29.2
31	-2	-7.4	-10	-4	-7.8	-11
32	-4	-6.2	-8.8	-4	-4.4	-5.6
33	0.2	1.6	0.2	0.4	2.2	1.4
34	2.6	1.2	-0.8	1.2	2.4	0.4
35	5	5.6	5.2	3	5.2	4.4
36	4.4	5.8	6.2	4.8	8.6	11.4
37	7.2	8.8	9.6	6.4	10.6	14.2
38	6.4	7	8	4.8	6	7
39	1.4	1	1.4	1.8	2	2.8

Gage Number	Ctr P3 Truck Weight (pounds) 23040	35980	46420	Ctr P4 Truck Weight (pounds) 23040	35980	46420
1	0.4	-1.6	-1.2	0.2	-0.8	0.4
2	0.6	0.6	0.4	-0.2	1.8	1.2
3	-1.4	-0.6	-1.2	-1.2	-0.8	0.4
4	-0.8	-1.4	-1.4	-0.4	-0.2	-0.2
5	-1.6	-4.6	-6.6	-1.8	-1.8	-2.8
6	-2.6	-7.2	-11	-1.8	-3.6	-5
7	1	0.8	0.8	0	0.4	0.4
8	2	2.8	2.8	0	0.4	1.4
9	1.6	3	2	0.8	1	1
10	2.6	3.4	4	0.8	2.2	1
11	-2.4	-2.4	-3.4	-1.2	-0.2	-0.2
12	-3.4	-3.6	-5.2	-2.2	-1.8	-1.6
13	0.6	2.8	2.2	-0.2	0.4	1.6
14	1.2	4	4.6	0.6	2	2.8
15	5	10.6	12.8	2	4.8	6.4
16	0.4	1.6	-0.4	0.2	0.8	0.8
17	-2.6	-2.4	-4	-0.8	-0.2	-1
18	1.8	4.4	5.8	1.4	2.2	3.4
19	1.2	1.8	-0.8	1.6	0.4	-0.4
20	0.8	1	-1.6	-0.6	1	0.2
21	-2	-4.6	-7	0	-1.8	-1
22	-0.8	-1.4	-4	0.6	-0.2	0
23	-0.2	-0.6	-1.8	0.4	0.2	0.6
24	1.4	1.2	-0.2	1.2	1.6	1.4
25	-2.4	-3.6	-8	-0.2	-0.8	-2
26	-3.4	-7.6	-11.2	-1.2	-2.8	-2.6
27	3.6	6.8	7.4	1.8	2.4	3.2
28	1.2	4	5.2	0.6	2	3.6
29	-3.2	-3.8	-5.8	-0.6	-0.4	0.6
30	10	18.4	23.8	3	6.2	9.4
31	-3	-6.2	-10	-1	-1.6	-1
32	-3	-5.6	-10.4	-1	-1.8	-1.2
33	1.6	2.8	1.6	-0.2	2.4	3.8
34	1.8	1.6	-1.4	0.4	0.8	1.8
35	7	11.8	12.6	2	5.4	6.8
36	5.2	8.4	9.6	1.6	3.2	6.8
37	5.6	8.4	9.8	4.8	2.2	6.4
38	8.2	14	17	2.6	5	8
39	2.2	3	3.2	0.6	2	4.6

APPENDIX C

Diagram Detailing Transducers Locations

Load: Empty Half Full
Midspan
North
Straddle: □
Centered: □
South
Tension □
Compression □
1
2
3
4
x